



**HAL**  
open science

## Metal–Organic Frameworks for Water Desalination

Subhajit Dutta, Roberto Fernández de Luis, Joanna Goscianska, Aude Demessence, Romy Ettliger, Stefan Wuttke

► **To cite this version:**

Subhajit Dutta, Roberto Fernández de Luis, Joanna Goscianska, Aude Demessence, Romy Ettliger, et al.. Metal–Organic Frameworks for Water Desalination. *Advanced Functional Materials*, 2023, 10.1002/adfm.202304790 . hal-04285754

**HAL Id: hal-04285754**

**<https://hal.science/hal-04285754>**

Submitted on 14 Nov 2023

**HAL** is a multi-disciplinary open access archive for the deposit and dissemination of scientific research documents, whether they are published or not. The documents may come from teaching and research institutions in France or abroad, or from public or private research centers.

L'archive ouverte pluridisciplinaire **HAL**, est destinée au dépôt et à la diffusion de documents scientifiques de niveau recherche, publiés ou non, émanant des établissements d'enseignement et de recherche français ou étrangers, des laboratoires publics ou privés.

# Metal–Organic Frameworks for Water Desalination

Subhajit Dutta,\* Roberto Fernández de Luis, Joanna Goscianska, Aude Demessence, Romy Ettlenger, and Stefan Wuttke\*

Rapid industrialization and ever-increasing global population culminate in continuous upsurge in freshwater crisis worldwide. The most reliable and promising solution to this crisis is utilizing sea-water as the freshwater source, and desalination technologies pave the way for efficient production of freshwater from sea-water. In this regard, membrane-based desalination method comes forth owing to its' efficient separation, operational ease, and low-energy consumption. Metal–organic frameworks (MOFs), the most explored crystalline porous materials, show tremendous promise as membrane-materials for desalination owing to their structural diversity, tunability, and porous voids which provide secondary water channels. Given significant advances are made in MOF-materials for desalination in the past few years, it is crucial to systematically summarize the recent progress and development of this field. In this review, a brief overview of various saline water systems and prerequisites for desalination are first presented. Then, advanced fabrication strategies MOF-membranes followed by the recent progress in MOF-materials for various desalination processes such as reverse osmosis and forward osmosis are systematically summarized. Finally, the authors' perspectives on the unsolved scientific and technical challenges and opportunities for MOF-integrated membranes toward real-world implementation are proposed. With further systematic development, MOF-materials promise to provide an ideal platform for next-generation desalination technology.

the era of technology and overpopulation, human civilization is facing a “never seen before” crisis as a consequence of man-induced activities since the advent of the industrial revolution that has brought about a profound negative impact on the Earth's ecosystem. Unfortunately, in the need to cope up with the ever-increasing demand of necessary goods in the modern society, not only have natural resources been over-exploited but also enormous amounts of hazardous wastes have been released.<sup>[4–7]</sup> This has a direct impact on the Earth's water system: presently nearly 50% of the world's population is living under water-stressed conditions (Figure 1). The gravity of the problem is so severe that it is recognized as one of the main goals of the Sustainable Development Agenda of the United Nations.<sup>[8–10]</sup> According to United Nations estimates, the global population will reach ≈10 billion by 2050, and as many as one billion people may face extreme difficulty accessing clean water even by 2025.<sup>[11]</sup> Hence, harvesting drinkable freshwater from groundwater sources as well as the desalination of seawater prevails, a priori, as a convenient and sustainable approach to mitigate the world's water crisis.<sup>[12–14]</sup> In particular, desalination has emerged as the most efficient and globally affordable solution for the intensifying water scarcity and accounts for ≈53% of today's global drinking water.<sup>[15,16]</sup> Desalination can be defined as


## 1. Introduction

Water is the most essential resource for all living beings. Although water covers nearly 71% of the earth's surface, only 0.5% of it is freshwater and can be used for drinking.<sup>[1–3]</sup> Living in

emerged as the most efficient and globally affordable solution for the intensifying water scarcity and accounts for ≈53% of today's global drinking water.<sup>[15,16]</sup> Desalination can be defined as

S. Dutta, R. F. de Luis, S. Wuttke  
BCMaterials  
Basque Center for Materials  
Applications and Nanostructures  
UPV/EHU Science Park, Leioa 48950, Spain  
E-mail: subhajit.dutta@bcmaterials.net; stefan.wuttke@bcmaterials.net

J. Goscianska  
Faculty of Chemistry  
Adam Mickiewicz University  
Poznan 61-614, Poland  
A. Demessence  
Univ Lyon  
Université Claude Bernard Lyon 1  
CNRS  
IRCELYON UMR 5256  
Villeurbanne 69626, France  
R. Ettlenger  
School of Chemistry  
University of St. Andrews  
St. Andrews KY16 9ST, UK  
S. Wuttke  
IKERBASQUE  
Basque Foundation for Science  
Bilbao 48009, Spain

 The ORCID identification number(s) for the author(s) of this article can be found under <https://doi.org/10.1002/adfm.202304790>

© 2023 The Authors. Advanced Functional Materials published by Wiley-VCH GmbH. This is an open access article under the terms of the Creative Commons Attribution License, which permits use, distribution and reproduction in any medium, provided the original work is properly cited.

The copyright line for this article was changed on 27 October 2023 after original online publication.

DOI: 10.1002/adfm.202304790

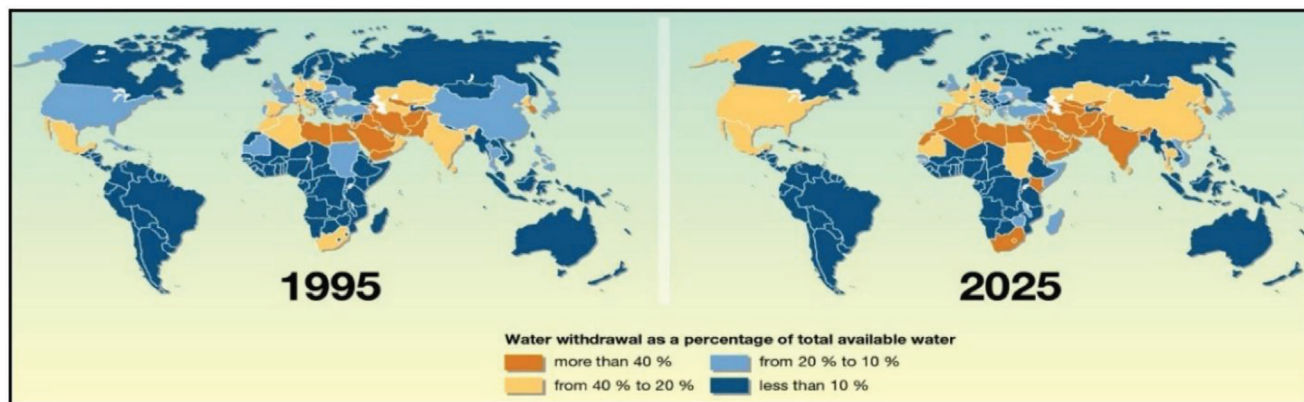


Figure 1. Comparison of global water crisis. Reproduced with permission.<sup>[199]</sup> Copyright 2017, Elsevier.

a method to separate salts and minerals from various saline water sources such as sea water, brackish water, industrial feed and process water, and waste water. Desalination technologies have advanced significantly since the installation of the first desalination plant in 1928, with the inaugural multi-effect distillation (MED) plant in 1930, the first multi-stage flash (MSF) distillation plant in 1957, and the first reverse osmosis (RO) plant in 1965.<sup>[17]</sup> Owing to the widespread availability of seawater and brackish water, desalinated water production can be easily integrated with the existing water supply systems globally. This accounts for more than 16 500 installed desalination plants globally (till February 2020) with freshwater production capacities of 97.2 million m<sup>3</sup> per day.<sup>[17–20]</sup> Till date, the research activities continue to improve the energy-economic aspects and ecological footprints reduction toward freshwater production, especially via membrane-based desalination processes such as reverse osmosis.

There are two prime methods for the desalination process: 1) thermal or distillation desalination and 2) membrane-based desalination.<sup>[16]</sup> These two methods as a whole contribute more than 90% of freshwater production via desalination processes. Thermal desalination technology involves boiling saline water to obtain pure water vapor. Particularly, evaporation processes such as multi-effect distillation and multi-stage flash are widely used to generate fresh water.<sup>[21–23]</sup> However, the thermal desalination processes render high energy-footprints as such processes require a minimum of 2260 kJ kg<sup>−1</sup> energy as latent heat for the vaporization of sub-cooled water.<sup>[24]</sup> In contrast to this, membrane-based desalination methods gained both scientific and engineering interest over the past decade owing to their lower energy consumption and better efficiency compared to the contemporary technologies. Membrane-based techniques, such as reverse osmosis, involve a much lower energy consumption (3.6–5.7 kWh) than thermal processes multi-stage flash (23.9–96 kWh) and multi-effect distillation (26.4–36.7 kWh) to produce one cubic meter of clean water including pre-treatment, brine disposal, and water transport energy requirements.<sup>[25,26]</sup>

The state-of-the-art reverse osmosis membranes include the thin film composites (TFCs) membranes, fabricated from interfacial polymerization of trimesoylchloride and m-phenylenediamine.<sup>[27,28]</sup> Further, nanoparticles of titanium dioxide, zeolite, and silica were introduced into thin film composites as membrane fillers to enhance the separation performance (i.e.,

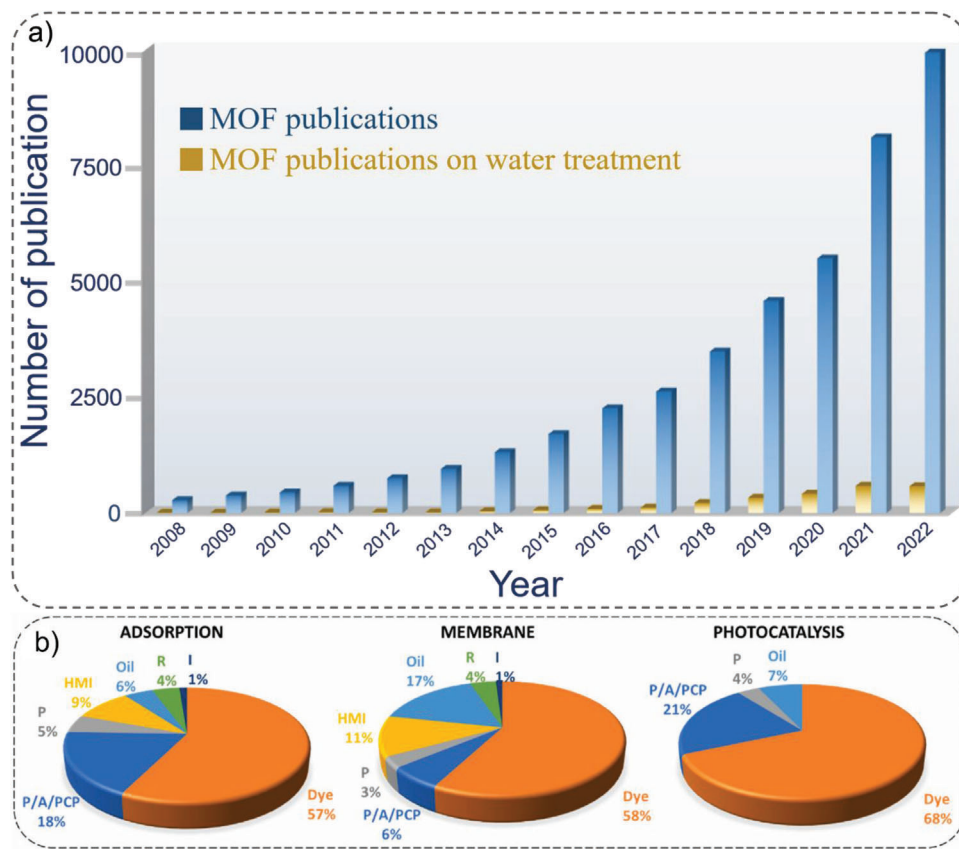
high flux and high rejection), resulting in thin film nanocomposites membranes.<sup>[29–45]</sup> However, these membranes often suffer from major limitations such as lower permeability, poor selectivity, and multistep fabrication. Depending on the source water, a broad range of different key contaminants have to be filtered with high efficiency, including boric acid from seawater, microbial pathogens, and micropollutants from surface waters or municipal wastewaters, drilling fluid additives from shale-gas produced water and toxic metals from coal-fired power plant flue gas desulfurization (Table 1). Therefore, the incorporation of functional and tunable porous materials as fillers to improve the physicochemical properties of the membrane is considered as one of the most promising solutions and becomes a research priority.

Herein, metal–organic frameworks (MOFs) membranes and their integration as novel membrane materials have created tremendous scientific interest in water desalination applications.<sup>[46–50]</sup> MOFs are crystalline solid porous materials having potential voids, fabricated from multi-dentate organic ligands and metal ions/clusters which further extend in an infinite periodic manner to structure a framework.<sup>[51,52]</sup> MOFs have come forth as the next-generation inorganic–organic hybrid porous materials for environmental nanotechnologies because of their superior physicochemical properties along with their highly tunable porous architectures, high surface areas, ease in functionalization, and so on. The last two decades have witnessed tremendous research growth in the field of MOFs and their extraordinary potential toward various on-demand applications including gas adsorption and separation, sensing, heterogeneous catalysis, ion-conduction, drugs delivery, water purification, and water harvesting.<sup>[53–75]</sup> The exponential growth in the number of MOF publications is testimony of their scientific popularity and widespread potential applicability (Scheme 1a). In particular, MOFs are considered as the most promising platform for water treatment because of their structural constructibility with molecular precision along with control over pore dimensions and functionalization which hold key importance in size and shape selectivity toward incoming guest molecules (Scheme 1b).<sup>[76–78]</sup> Compared to the traditional inorganic materials-based membranes with rigid structures, which often suffer from segregation and pore-blocking, MOFs-incorporated membranes have shown to improve material compatibility with enhanced membrane

**Table 1.** Classification of different natural saline and waste-waters.

Source water	Key contaminants	Treatment objectives	Membrane technologies <sup>a)</sup>	Problems and challenges
Natural waters				
Seawater	Boric acid (affects crop health), divalent cations (cause scaling issues)	Reduce salinity	<ul style="list-style-type: none"> <li>Pre-treatment: microfiltration and ultrafiltration</li> <li>Desalination: reverse osmosis</li> </ul>	<ul style="list-style-type: none"> <li>Energy of desalination</li> <li>Ecological impact of seawater intake and brine discharge</li> </ul>
Brackish (saline) groundwater	Divalent cations	Reduce salinity	<ul style="list-style-type: none"> <li>Pre-treatment: MF and UF</li> <li>Desalination: RO and electro dialysis</li> </ul>	<ul style="list-style-type: none"> <li>Inland discharge of saline brine</li> </ul>
Surface waters	Natural organic matter (precursor for disinfection by-products), microbial pathogens, micropollutants, and algal toxins	<ul style="list-style-type: none"> <li>Remove particles and microbial pathogens</li> <li>Reduce natural organic matter</li> </ul>	<ul style="list-style-type: none"> <li>MF, UF, nanofiltration and RO</li> </ul>	<ul style="list-style-type: none"> <li>High fouling potential</li> <li>Formation of toxic disinfection by-products during oxidative disinfection</li> </ul>
Fresh groundwater	Natural arsenic, nitrates, iron, and manganese (staining issues) and divalent cations	<ul style="list-style-type: none"> <li>Reduce nitrate, iron, manganese, and/or scale-forming ions</li> </ul>	<ul style="list-style-type: none"> <li>MF, UF, NF, and RO</li> </ul>	<ul style="list-style-type: none"> <li>Seawater intrusion for aquifers near ocean</li> <li>Aquifer over-exploitation</li> </ul>
Wastewaters				
Municipal wastewater	Microbial pathogens, micropollutants, phosphates (algal bloom concerns), and ammonia	<ul style="list-style-type: none"> <li>Degrade organic matter</li> <li>Remove or inactivate pathogens</li> <li>Remove nutrients (that is, nitrogen and phosphate)</li> </ul>	<ul style="list-style-type: none"> <li>MF, UF, NF, and RO</li> </ul>	<ul style="list-style-type: none"> <li>Requirements for potable reuse</li> <li>Large footprint</li> <li>Odour of conventional treatment plants</li> <li>High membrane-fouling potential</li> </ul>
Shale-gas produced water	Drilling fluid additives (for example, surfactants, oxidants, strong acids), oil and grease, radium, and divalent cations	<ul style="list-style-type: none"> <li>Drilling reuse: remove suspended solids and scalants</li> <li>Disposal: remove oily compounds and reduce salinity</li> </ul>	<ul style="list-style-type: none"> <li>Drilling reuse: MF and UF</li> <li>Desalination: NF, RO (low-salinity), forward osmosis, and membrane distillation</li> </ul>	<ul style="list-style-type: none"> <li>Large water consumption</li> <li>High total dissolved solids</li> <li>Fluctuating water quantity and quality</li> <li>Regulations over disposal of high membrane-fouling potential</li> </ul>
Coal-fired power plant flue gas desulfurization	Toxic metals (e.g., arsenic, selenium, and mercury), ammonia, and organic acids	Remove dissolved toxic metals and reduce salinity	MF, UF, NF, RO, FO, and MD	Potential zero liquid discharge requirements

<sup>a)</sup> MF: membrane filtration; RO: reverse osmosis; UF: ultrafiltration; NF: nanofiltration; FO: forward osmosis; MD: membrane distillation.



**Scheme 1.** a) Comparison of the increasing number of articles with the keywords “Metal–organic Frameworks,” “Metal–organic Frameworks water treatment” (source: Web of Science). b) The distribution of MOF publications on wastewater treatment: R: Radioactive, I: Insecticides, HMI: Heavy Metal Ions, P: Pesticides, P/A/PCP: Pharmaceutical or Antibiotics or Personal Care Products. Reproduced with permission.<sup>[226]</sup> Copyright 2022, Elsevier.

permeability and selectivity. Hence, the utilization of MOFs as fillers in both mixed matrix membranes (MMMs) and thin film nanocomposites-membranes is rapidly developing toward water filtration and water-treatment applications.<sup>[79,80]</sup>

In this review, we aim to make a comprehensive summary of the state-of-the-art development of MOFs and MOF-based membranes for highly demanding water desalination applications (Scheme 2). In the subsequent sections, we give an overview of various saline water systems, separation mechanisms for desalination, and structural requirements for desalination. Concomitantly, different synthetic strategies to fabricate MOF-membrane materials are highlighted. Afterward, a detailed discussion regarding the key role of MOFs toward desalination and mechanistic insights is provided. Finally, we underline the current challenges, windows of opportunities, and future perspective of these promising materials for water desalination.

## 2. Classification of Saline Water

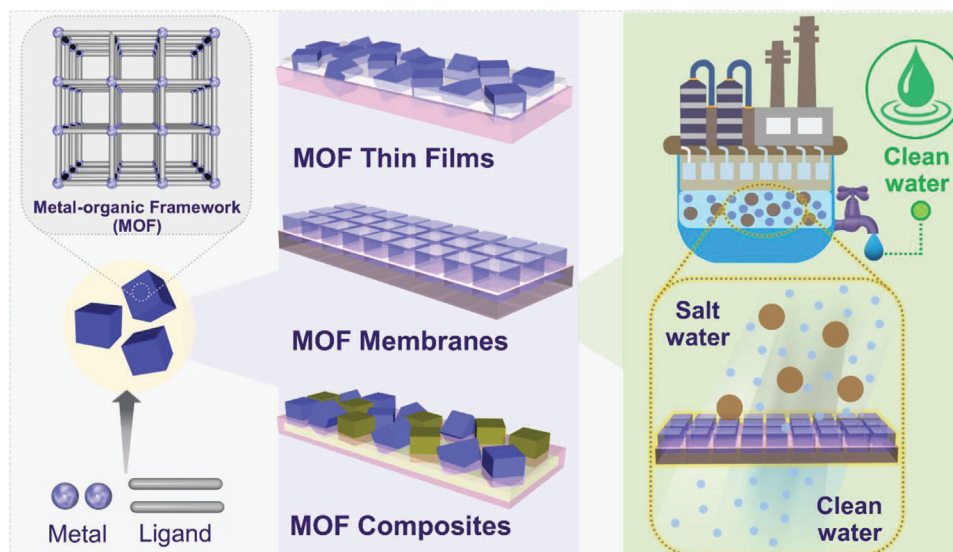
Typically, the term “salinity” is attributed to the salt concentrations in water or soils. Depending upon their nature, salinity can be categorized into three classes: primary salinity (known as natural salinity), secondary salinity (known as dryland salinity), and tertiary salinity (known as irrigation salinity).<sup>[81]</sup> Although a small amount of dissolved salts in natural waterways is essential for

the maintenance of aquatic symbiosis and the survival of marine life, increased salinity levels are hazardous to many plants and animals. Depending upon the level of salinity, natural water bodies can be classified into six major categories ranging from non-saline water with a salt concentration as low as  $<500 \text{ mg L}^{-1}$  (drinking water) up to brine with  $>45,000 \text{ mg L}^{-1}$  (Table 2).

In parallel, salinity can be considered as an opportunity to concentrate certain valuable resources. So, desalination can be understood as a process able to generate fresh drinkable water, and in parallel, a brine reject with valuable elements such as uranium or boron is concentrated. Going a step forward, by developing an element selective desalination, a revalorization and metal-concentration process can be developed. The application of the background obtained from materials and membrane sciences applied to desalination, is still to be adapted to the revalorization of high saline/brine waters.<sup>[82–86]</sup> This will bring the opportunity to access drinkable water and critical resources from lithium-rich brines, mining acid water or drainages, or high saline industrial effluents, as these ones arising from phosphogypsum deposits.

## 3. Key Mechanisms for Desalination

A clear understanding of the mechanism of any sorption or separation process holds the key to developing and exploring the potential of novel materials. The mechanisms for water



**Scheme 2.** Schematic illustration of MOFs and various types of MOF-based membranes for water desalination.

desalination can be broadly classified into three classes and will be discussed briefly (**Figure 2**): 1) desalination via phase change, 2) desalination via short-range interactions, and 3) desalination via electrostatic interactions.<sup>[26]</sup>

### 3.1. Desalination Via Phase Change

Desalination via phase change is regarded as the most traditional technique. In particular, the liquid–vapor phase transition method is the most widely utilized method for desalination in which the feedwater undergoes vaporization to form vapor, and in the process, the salt gets separated.<sup>[25]</sup> Desalination techniques such as multi-effect distillation and multi-stage flash are primarily based on the liquid–vapor phase transition method. Next to it, solidification or freezing of the feedwater to form ice is another efficient method to separate salt from water as the salt conversely remains in the liquid phase. Freezing desalination has been considered a more efficient method than evaporation-based methods owing to its' lower energy footprints. From the thermodynamic point of view, the latent heat of vaporization and freezing of water are 2256 and 330 kJ kg<sup>-1</sup>, respectively. The energy requirement for freezing desalination process is almost 1/7th of the energy requirement for evaporation-based desalination processes.<sup>[87]</sup> However, this method also suffers from chal-

lenges in the infrastructure design and implementation to handle the complexity of the ice and water mixture and purification of contaminated water which has limited its commercialization globally.<sup>[87–89]</sup>

### 3.2. Desalination Via Short-Range Interactions

Short-range molecular interactions between the ions or water molecules with the sorbent material have shown tremendous promise in developing next generation desalination materials. They include steric, dipole, and electrostatic interactions and dispersion. These interactions can promote the desalination process via preferential movement of the ions or water molecules through the sorbent material or via chelation and absorption/adsorption of the ions. Although chelation and adsorption are regarded as the more suitable method for the sorption of trace metals, separation via transportation through a selective material or membrane has been utilized in well-established techniques such as reverse osmosis.<sup>[90,91]</sup> From the materials' point of view, it can be classified into two: flexible materials (e.g., polymers) and rigid materials (inorganics). The function of flexible materials typically depends on selective sorption and transport, whereas the rigid material-based separation involves steric exclusion-driven molecular sieving. In the case of polymeric reverse osmosis

**Table 2.** Classification of saline waters.

Water class	Electrical conductivity [dS m <sup>-1</sup> ]	Salt concentration [mg L <sup>-1</sup> ]	Type of water
Non-saline	<0.7	<500	Drinking and irrigation water
Slightly saline	0.7–2	500–1500	Irrigation water
Moderately saline	2–10	1500–7000	Primary drainage water and groundwater
Highly saline	10–25	7000–15 000	Secondary drainage water and groundwater
Very highly saline	–	15 000–35 000	Very saline groundwater
Brine	>45	>45 000	Seawater

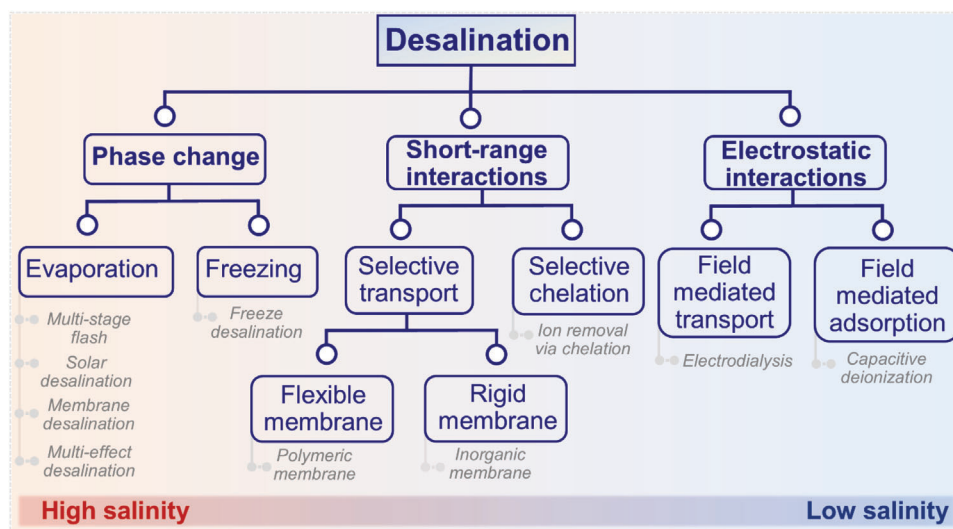


**Figure 2.** Details of different mechanisms involved in desalination and their utilizations in different processes.

membranes, the selectivity arises from the higher diffusivity of water molecules compared to ions, while rigid membranes primarily work as molecular sieves to separate the larger hydrated salt ions ( $\approx 7\text{--}8\text{ \AA}$ ) from the smaller water molecules ( $\approx 3.3\text{ \AA}$ ).

### 3.3. Desalination Via Electrostatic Interactions

Desalination via electrostatic interactions involves electro-kinetic methods where electric fields are used for the depletion, accumulation, and transportation of ions. The potential difference between the electronically polarized ions and neutral water molecules enables the employment of electrostatic fields to selectively exert ions from water.<sup>[92]</sup> Hence, a charged surface attracts ions with opposite charges while repelling ions having the same charges, resulting in the formation of electric double layers. Therefore, the dissolved ions can be selectively adsorbed on the charged surfaces or be dictated by electrostatic interactions for preferential transportation through membranes. Such methods are widely utilized in techniques such as capacitive deionization and electrodialysis for desalination.

## 4. Prerequisites for Desalination

Typically, natural water bodies contain various types of monovalent and multivalent salts, for example, NaCl, KCl,  $\text{MgSO}_4$ ,  $\text{MgCl}_2$ ,  $\text{CaCO}_3$ , and  $\text{Na}_2\text{SO}_4$ , which are the prime targets for desalination processes. To desalinate these ions, different kinds of membranes have been utilized. Depending upon their working principal, these membranes can be divided into three categories and will be discussed in the following: 1) external pressure-driven membrane desalination, 2) osmotic pressure driven membrane desalination, and 3) thermal-driven membrane desalination.

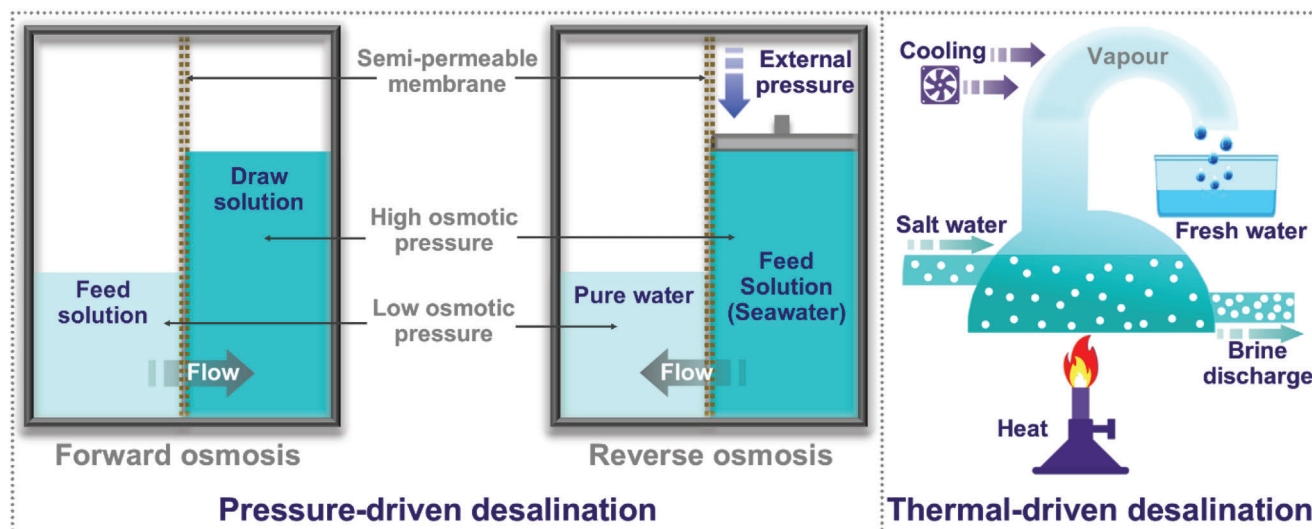
### 4.1. External Pressure-Driven Desalination

In pressure-driven desalination processes such as reverse osmosis, nanofiltration, ultrafiltration, and microfiltration, pressure is applied on the feedstock from one end of the membrane

which acts as a driving force to separate the ions from the water (Scheme 3). Among them, reverse osmosis has been the most popular and widely used method in desalination while nanofiltration is generally employed for water treatment with lesser salt content such as brackish water and industrial water.<sup>[93,94]</sup> As the name indicates, reverse osmosis processes are engaged with the difference in osmotic pressure between pure water and highly concentrated saline water. In this process, water is forced in a reverse manner when the applied external pressure is higher than the osmotic pressure of the membrane. Contrarily, microfiltration processes operate through convective transport and solution-diffusion as in the process, the salt concentration is reduced. In general, the thin film composites for both reverse osmosis and nanofiltration processes consist of a selective thin layer ( $\approx 0.2\text{ }\mu\text{m}$ ) and a microporous layer ( $40\text{--}50\text{ }\mu\text{m}$ ). The thin layers are typically based on polyamides, fabricated from polycondensation of different amine monomers.<sup>[95]</sup> These thin layers for reverse osmosis are densely packed whereas the thin layers for nanofiltration membranes are generally less dense. Moreover, these thin layers can feature a range of porous architecture (pores in the range of  $\approx 1\text{--}10\text{ nm}$ ). However, these thin layers often suffer from lower selectivity and permeability at high salt rejection. Hence, emphasis should be given to the hydrophilicity of these dense thin layer for both reverse osmosis and nanofiltration membranes in order to facilitate the salt retention and movement of the water molecules.

### 4.2. Osmotic Pressure Driven Desalination

Forward osmosis is one of the emerging desalination membrane technologies which operates via simple osmotic pressure difference between feed solution and draw solution. In this method, the osmotic pressure difference acts as the driving force to transport the solution from the feed solution (lower osmotic pressure) to the draw solution (high osmotic pressure), resulting in the dilution of the draw solution (Scheme 3).<sup>[96]</sup> Alike to reverse osmosis and nanofiltration membranes, most of the



**Scheme 3.** Schematic illustration of various types of working principals for desalination.

forward osmosis membranes are thin film composite membranes with densely packed layers without any significant pores, which provide the ideal surface for effective separation of the salts from water. Hence, the effectivity of forward osmosis membranes depends on the hydrophilicity and permeability of the membrane materials. However, higher solute aggregation on the membrane is the major drawback of forward osmosis membranes which limits their long-term utilization. In this regard, the fabrication of forward osmosis membranes with different porous materials with high porosity, thinner thickness, and low tortuosity, is regarded as one of the best methods to address this issue.<sup>[97]</sup>

### 4.3. Thermal Driven Desalination

Membrane distillation is the most efficient thermal-driven desalination process in which heat is supplied to the feed solution to generate vapor pressure driven flux, and the membranes allow transportation of the vapor over water through it (Scheme 3).<sup>[98]</sup> The most important aspect of an efficient membrane distillation membrane is the hydrophobicity of the synthetic materials in order to prevent humidity accumulation on the surfaces. In addition, structural features such as microporosity (in the range of 0.1–1  $\mu\text{m}$ ), low resistance to mass transfer, good thermal stability, and low thermal conductivity are the prime requirements to fabricate membrane for membrane distillation.<sup>[99]</sup> Another important aspect to maximize the mass transfer of heat is an optimum membrane thickness in the range of 30–60  $\mu\text{m}$ .<sup>[100]</sup>

## 5. Key Characteristics of MOF-Based Materials for Desalination

There are several important factors that should be considered in designing an efficient desalination membrane: choice of membrane materials, module configuration, high flux and solute rejection, mechanical and thermal stability, physicochemical stability, cost-effectiveness, processability at the large scale, and operational complexity. Consequently, the selection of MOFs for real-world liquid separation should be based on the aforementioned

factors as well as the chemical stability and the separation potential of the chosen MOF. The filtration performance of the resulting MOF-based mixed matrix membranes (MMMs) is crucial in screening MOFs for water desalination. Typically, liquid filtrations are directed by the flow pressure on the feed, which imparts force on smaller solutes to permeate through the membrane and for subsequent rejection of species larger than the pore diameter. MOFs generally can be tailor-made to have non-deformable pore windows which can help in selective permeability driven molecular sieving. In the following section, the major criteria for MOFs and MOF-based membranes, namely their water stability, pore size and aperture, dispersibility, particle size, and hydrophobicity/hydrophilicity for desalination will be discussed.

### 5.1. High Water Stability

Clearly, water stability is one of the most important properties for any material toward practical applicability.<sup>[79]</sup> Particularly, hydrolytic stability is the primary criterion for MOFs to be used for water treatment. In addition, as different natural water systems are constituted of diverse chemical compositions, the selected MOF structures are required to retain their structural integrity even in harsh chemical conditions, such as acidity, basicity, and metal ions exchange. Although, not all of the >90 000 reported MOF structures<sup>[57,101]</sup> exhibit excellent water stability but rather tend to undergo irreversible structural degradation in hydrolytic or humid conditions, systematic evaluation of the available data revealed three main strategies to synthesize water-stable MOFs: 1) formation of metal–carboxylate bonds to construct frameworks with high-valent metal ions, 2) creation of metal–azolate bonds, and 3) hydrophobic shielding of the metal ions via functional groups or hydrophobic pore surfaces. Thus, to meet the demand of desalination treatment, utilization of metal–carboxylate frameworks and metal–azolate frameworks is found to be most beneficial.<sup>[102,103]</sup> In this regard, it is noteworthy to mention that significant scientific attention has been devoted to developing water stable MOFs during the last decade. Following this path, a



range of water stable MOFs has been reported in literature: 1) Zr-based UiO-66 series, PCN-228/–229/–230, PCN-521, PCN-777, MOF-808, NU-1000, NU-1105, MIL-160, MIL-163, and FJI-H6; 2) In-based MIL-68, JLU-Liu18, and InPCF-1; 3) Hf-based FJI-H7 and PCN-523; 4) Al-based MIL-121, CAU-10, and so on, are among them.<sup>[105]</sup> Depending upon their pore architecture and the demand of desalination applications, these MOFs can be utilized to fabricate efficient desalination material

## 5.2. Pore Size and Pore Aperture

The pore size and pore aperture of porous materials are fundamental properties for efficient desalination performance. The pore dimensions of porous materials typically govern the extent of water flux through the material along with its salt rejection ability. The key to get an efficient separation process is knowing the size of the target pollutants because, in theory, a membrane works as a selective barrier. In contrast to other porous materials, the reticular chemistry of MOFs has enabled control over framework dimensionalities and topologies via tailored designing and judicious choice of metal ions and organic linkers to fabricate MOFs with desired properties.<sup>[104]</sup> To this end, microporous or ultra-microporous MOFs with small pore dimensions are considered to be the perfect match for water desalination as they can impart additional separation barrier to the ions and can also act as a water channel toward efficient desalination performance. For example, microporous water-stable MOFs such as UiO-66(Zr) (6.0 Å), MIL-53(Al/Cr) (8.5 Å), ZIF-8(Zn) (3.4 Å), and ZIF-90(Zn) (3.5 Å) feature smaller pore window than that of hydrated diameter for most of the dissolved ions.<sup>[105]</sup> In this regard, MOFs that are built from robust structure with higher valent metal ions (Zr<sup>+4</sup>, Al<sup>+3</sup> etc.) should be given priority considering their higher structural and physiochemical stability. Moreover, the integration of microporous MOFs into membranes turns out to enhance the membrane permeability as it can easily allow selective transportation of water molecules across the membrane layer, while simultaneously restricting the dissolved ions.<sup>[80,106–112]</sup>

## 5.3. Pore Space

One of the most advantageous properties of MOFs is their ability to encode the pore space with specific chemical groups via the pre- or post-synthetic modification of the inorganic and/or organic building blocks.<sup>[61,113]</sup> The precise control over the spatial and positional orientation of the installed functional groups can lead to diverse unique structural and physical properties, which make this material highly versatile and differentiate from the rest of the functional materials. Several strategies can be employed for pore space functionalization of MOFs, for example, functional-site cooperation, functional-site isolation, and functional-site coupling.<sup>[61]</sup> Moreover, such chemical encoding can render in improved adsorptive affinity toward targeted ions or higher controllability in migration of water molecules and metal ions along the porous channeled structure. For instance, presence of polar functional groups such as –COOH, –SO<sub>3</sub>, –PO<sub>3</sub>, and –OH can improve the desalination performance of the MOF material via preferential interactions with the incoming guest

ions. On the other hand, judicious choice of the organic building blocks can improve the compatibility with the polymer components during formation of the MOF–polymer composite to fabricate desalination membrane. Moreover, the chemical versatility of MOF pore space has enabled mimicking water (aquaporin) and metal–ion anisotropic channels of proteins<sup>[114]</sup> into the pore-channels,<sup>[115,116]</sup> leading to a fast and selective migration of water molecules and ions.<sup>[117–119]</sup> Defect engineering, particularly with M(IV) metal ions-based MOFs, has also shown promise as another alternative strategy to tune the selectivity of water and metal–ion migration based on their hydrodynamic radii in solution. Despite their chemical versatility, integration of MOF particles or MOF-layers into polymeric membranes is a mandate in order to utilize them as a functional porous matrix in water desalination systems. In addition, orientation of the MOF particles in the MOF-embedded membranes is also very important in achieving highest accessibility of the installed functionalities inside the pores of the MOFs for water desalination.<sup>[114,119]</sup>

## 5.4. Dispersibility

Apart from the stability and permeability of MOFs, dispersibility of the MOF particles in the resulting composite membrane is another important criterion for the overall performance. Although several MOFs have shown their compatibility with different polymer materials, a high mass concentration loading of MOFs with respect to the used polymer generally resulted in particle aggregation. This aggregation is primarily driven by the surface energy generated from strong van der Waals interactions between the individual MOF particles which get reduced after aggregation.<sup>[120]</sup> In this regard, the pre-dispersion approach has been proven to be beneficial where the MOF particles are dissolved in a solvent with lower viscosity followed by the introduction of the polymer solution. On the other hand, poor compatibility between the MOFs and the used polymer can often lead to cracks in the membrane, particularly, in case of high loading. This can be overcome by strategic modifications in the materials combination as well as the employed fabrication methods. For instance, Wang and co-workers established a thermally induced phase separation-hot pressing (TIPS-HoP) method for roll-to-roll production of MOF-membranes.<sup>[121]</sup> Utilizing this strategy, they have fabricated as many as ten different MOF-based MMMs with the highest MOF loading up to 86 wt%. Moreover, interfacial MOF formation on the membrane surface via methods such as layer-by-layer assembly or in situ self-assembly, has shown great promise to achieve higher dispersion of MOF particles on the membrane surface.<sup>[122,123]</sup> Apart from selecting the appropriate fabrication technique, surface modification of MOFs to introduce targeted functional groups has been also utilized to improve the dispersibility and reduce the extent of aggregation.<sup>[124–126]</sup>

## 5.5. Particle Size

The particle size of MOFs plays a key role in determining the resulting physicochemical properties as well as the interaction between the fillers and matrix materials. Several crucial properties of the membrane such as selective layer thickness, morphologies of the membrane, surface roughness, hydrophilicity,

and surface charge are primarily governed by the particle size of the fillers. In addition, particle size of the fillers also significantly affects the overall performance of the membranes. For example, utilization of large MOF particles can result in thicker selective layer of the membrane and enhanced water resistance of the material. Hence, control over particle size of the MOFs is very important to obtain desired property and performance of the selective layer.<sup>[127]</sup> Ideally, particle size should be <150 nm in order to obtain the best performance of the membrane. Typically, formation of MOF nanoparticles can be described via the LaMer model which describes the nucleation of nanoparticles as a function of concentration and reaction time. This involves four consecutive steps: 1) rapid enhancement of reactive monomer concentration in the reaction mixture, 2) homogenous nucleation outbreak because of exceeding reactive monomers concentration than that of critical nucleation concentration, 3) rapid decrease in reactive monomers concentration resulting in delayed nucleation events, and 4) extended growth of nanocrystals driven by saturation concentration of the reactive monomers.<sup>[128,129]</sup> According to the LaMer method, the short nucleation period is very much important to disassociated crystal nucleation from the crystal growth, which eventually results in uniform nanoparticle formation. To obtain uniform MOF nanoparticles in the range of 10–100 nm, the generation of a huge number of nuclei via nucleation outbreak and rapid termination of particle growth via decrease in the concentration of all precursors is crucial. Generally, MOF nanoparticle synthesis involves three main stages that require control: 1) rapid nucleation, 2) nanoreactor confinement, and 3) coordination modulation<sup>[58,62,130]</sup> followed by an accurate determination of the size distribution.<sup>[131,132]</sup>

### 5.6. Hydrophobicity/Hydrophilicity

The resulting hydrophilicity or hydrophobicity of a MOF structure is primarily governed by the nature of its organic ligand and the contribution of open metal sites. Therefore, a rational selection of the MOF building blocks can be fine-tuned with respect to the nature of the target analyte/species.<sup>[133,134]</sup> Although MOFs with higher hydrophobicity exhibit excellent separation performances for different organics, they often encounter difficulties upon integration into the polymers for water treatment applications. In such cases, hydrophobic MOFs were found to act adversely, resulting in less water permeability and overall efficiency. To this end, the incorporation of hydrophilic MOFs or MOFs with improved hydrophilicity is of great interest to optimize the overall performance of MOF-based composites for water desalination,<sup>[135]</sup> and several different strategies have been developed to date.<sup>[136–138]</sup> It should be noted that the hydrophobicity or hydrophilicity of the MOF-based composites or membranes can be monitored via controlling the functionalization of both the MOFs and the organic polymer building units. Hence, it is important to select an appropriate MOF with specific hydrophobic or hydrophilic properties for different water desalination membranes, for example, reverse osmosis and forward osmosis.

## 6. Design and Synthesis of MOF Membranes

The last decade witnessed significant growth in the design and development of water-stable MOF-based membranes for water

treatment applications (Figure 3). The ideal blend of appropriate MOF synthesis and membrane production is of paramount importance for fabrication of a stable MOF-based membrane. Broadly, their design strategies can be classified into two groups and they will be discussed here: 1) pure MOF membranes and 2) MOF-based composite membranes.

### 6.1. Pure MOF-Based Membranes

As indicated by the name, pure MOF membranes are fabricated from pristine crystalline MOF materials. In such membranes, the permeation selectivity and overall performance of the membrane are generally governed by the pore characteristics, such as the nature of building blocks, pore size, and pore aperture of the MOFs.<sup>[149]</sup> However, such membranes are often found to exhibit low mechanical strength, along with various structural defects, which limits their longer-term usability and commercial applications. MOF membranes can be fabricated via three different methods, namely direct growth method, secondary growth method, and layer by layer method.

#### 6.1.1. Direct Growth

In this method of membrane preparation, all the building components of the MOF and the support matrix are blended in a single precursor solution where the crystal nucleation, growth, and co-growth occur simultaneously (Figure 4). Hence, the growth of the MOF on the support surface happens in situ. Such direct growth methods can utilize unmodified supports as well as modified supports for the direct growth. In 2013, Qiu and co-workers described an efficient in situ direct growth strategy to fabricate a homochiral MOF membrane with cost-effective raw materials, high thermal stability, and an uncomplicated operational method.<sup>[150]</sup> Utilizing a nickel mesh substrate as both the nickel source and the unmodified supports material, they were able to grow the single crystals of the MOF around the nickel mesh. However, such direct growth strategy often suffers from limitations such as poor substrate bonding. In contrast, the application of modified supports for the direct growth approach offers enhanced heterogeneous nucleation and improved growth directionality of the MOF membranes. To this end, Huang and co-workers synthesized different crystalline zeolitic imidazolate framework (ZIF), ZIF-8 membranes via utilizing bio-inspired polydopamine to modify the support surface.<sup>[151]</sup> They modified the surface of a porous  $\alpha$ -Al<sub>2</sub>O<sub>3</sub> disk support with polydopamine, which resulted in a support surface without defects or cracks. Further, the support was found to have better attachments and promote nucleation and in situ growth for the ZIF materials. In addition, the ZIF membranes exhibited excellent separation performances toward seawater desalination with very high ion rejections of >99.8%.

#### 6.1.2. Secondary Growth

The secondary growth strategy involves the utilization of previously attached seed crystals upon which the growth of a membrane occurs (Figure 4). In comparison to direct growth, this

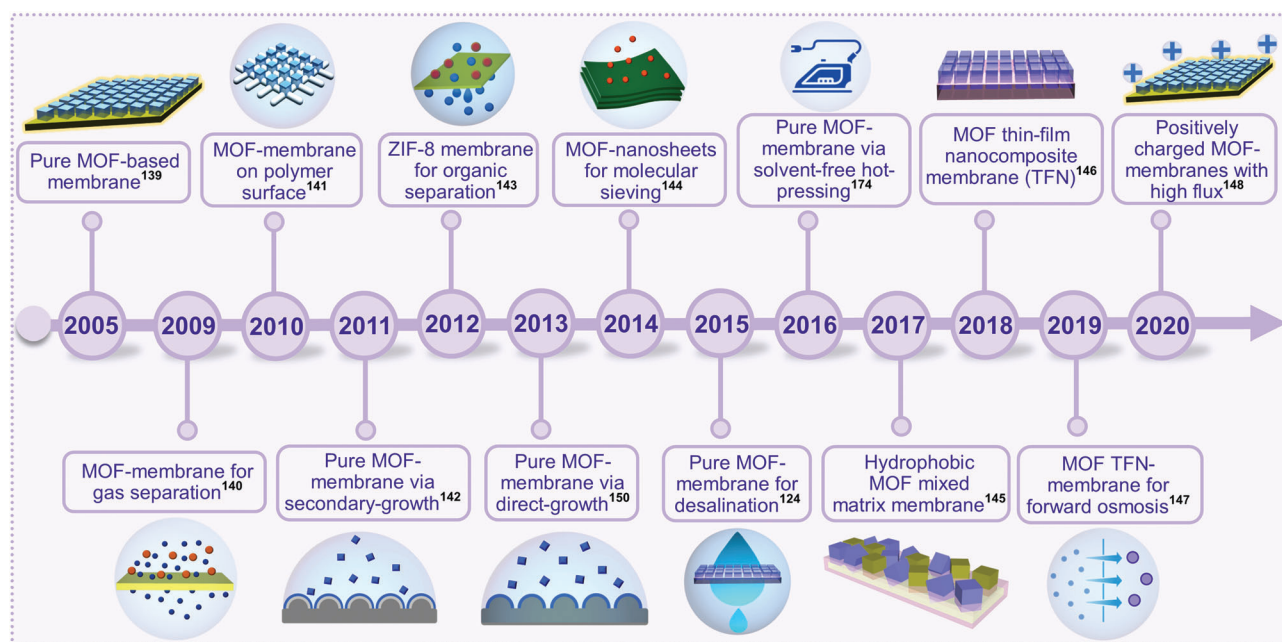


**Figure 3.** Timeline of advancements in MOF-membrane and wastewater treatment.<sup>[139–148]</sup>

strategy offers better control over crystal orientation and crack-free denser continuous membranes. For the secondary growth process, the interfacial attachment strength between the MOF crystals and the support surface plays a key role. To date, different strategies have been adapted to fabricate membranes via the secondary growth process. In this regard, Jin and co-workers developed a ZIF-300(Zn) membrane on an  $\text{Al}_2\text{O}_3$  substrate for the first time via the secondary growth method.<sup>[152]</sup> The integrated pure ZIF-300(Zn) membrane exhibited excellent size discrimination ability along with considerable water permeance ( $39.2 \text{ L m}^{-2} \text{ h}^{-1} \text{ bar}^{-1}$ ) and very good heavy metal ions rejection performance (99.21%). In another report, Pan and co-workers demonstrated the preparation of high-quality ZIF-8(Zn) membranes via hydrothermal seeded secondary growth method.<sup>[143]</sup> Utilizing ZIF-8 nanocrystals, a seed layer was first applied over the porous  $\alpha$ -alumina substrate, and after that, the seeded substrate was submerged in the ZIF-8(Zn) precursor solution to allow the formation of a dense ZIF-8(Zn) membrane via secondary growth method. This ZIF-8(Zn) membrane exhibited excellent chemical and thermal stability, reproducibility, and very good separation performance toward diverse propane/propylene mixtures. Interestingly, alike to direct growth, the seeding step in secondary growth could also be executed during the in situ growth process in which the porous support would act as the inorganic source and could form the seeding layer by reacting with the organic precursor. This process is known as reactive seeding. In this regard, Lee and co-workers established a MOF membrane based on an  $\alpha$ -alumina substrate as support and MIL-53(Al) via reactive seeding method (Figure 5a–e).<sup>[142]</sup> The reactive seeding method is proven to be beneficial to obtain uniformity, good orientation, and thin layers of the MOF membrane.

### 6.1.3. Layer-by-Layer Growth

Apart from direct growth and secondary growth method, the layer-by-layer growth method has also been utilized to fabricate MOF membranes. In this method, instead of mixing all the precursors, they are introduced one by one to the support material and allowed to form a layer. The layer formation process happens in a cyclic way in which the MOF membrane forms. In 2007, Shekha, Wöll and co-workers developed the first MOF-based thin film with HKUST-1(Cu) via layer-by-layer method (Figure 5f).<sup>[153]</sup> In 2015, Lei and co-workers demonstrated fabrication of multilayer Polyamide/ZIF-8 thin film nanocomposite membranes via layer-by-layer assembly approach.<sup>[154]</sup> The multilayer structure was constructed from a porous substrate, a Polyamide coating layer, and a ZIF-8 interlayer. Further, the as-synthesized membrane was found to exhibit excellent flux enhancement and rejection efficiency in nanofiltration application. In a recent report, Chen and co-workers have developed a new class of material, namely,  $\text{Fe}_3\text{O}_4@$ HKUST-1(Cu)/MIL-100 (Fe) via integrating the layer-by-layer method with the epitaxial growth method.<sup>[155]</sup>

## 6.2. MOF-Based Composite Membranes

MOF-based composite membranes are the most promising and widely utilized for water treatment applications. This class of membranes is fabricated via embedding MOF particles as porous fillers into a polymer matrix to form composite membranes. This is found to result in an improved trade-off between selectivity and permeability of the polymeric membranes along with enhanced thermal stability and mechanical strength of the overall

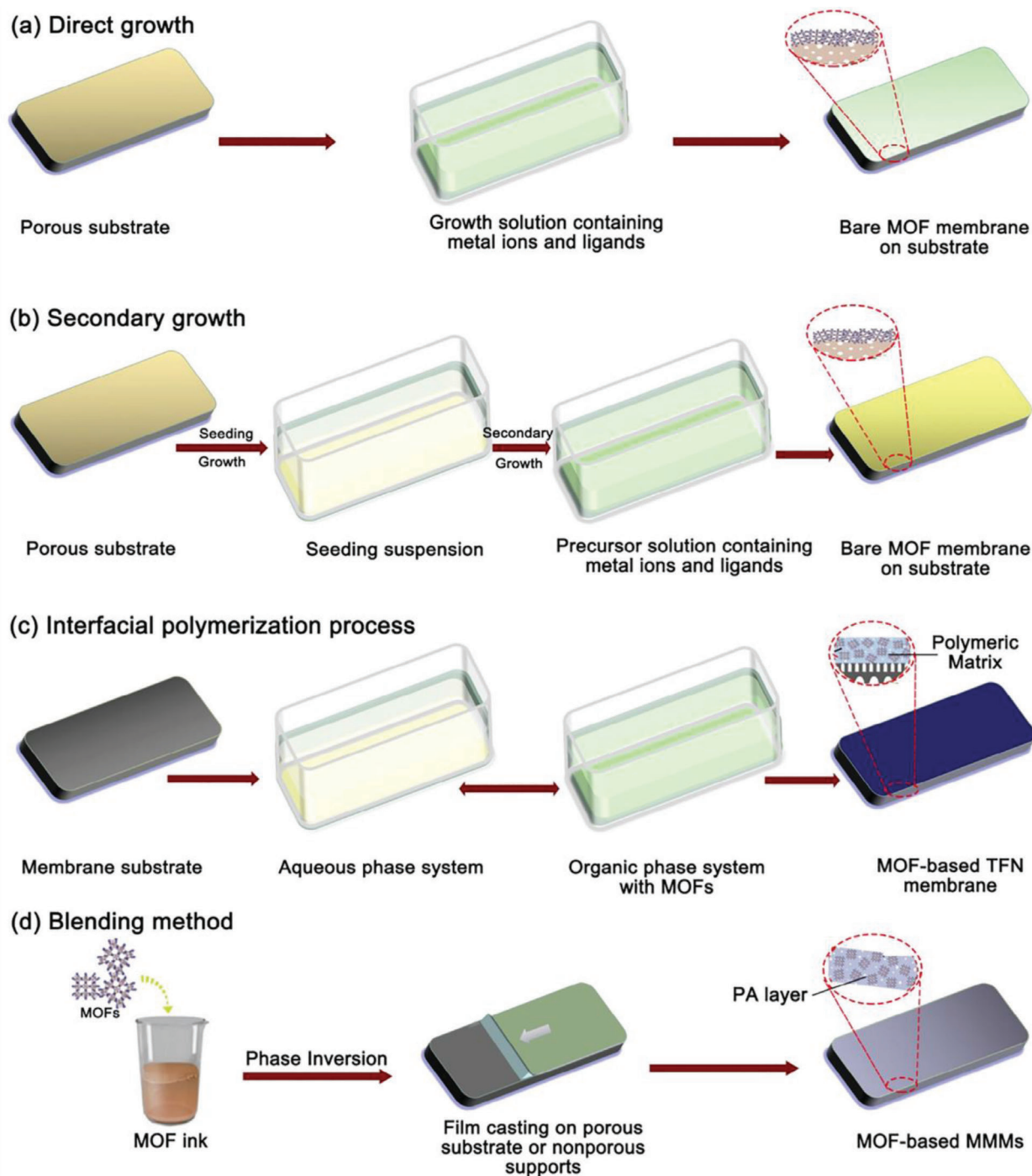


**Figure 4.** Different MOF-membrane fabrication strategies via direct growth method. Reproduced with permission.<sup>[49]</sup> Copyright 2020, Elsevier.

membrane. In the following section, a brief overview of design strategies of MOF-based composite membranes is presented.

### 6.2.1. Thin-Film Nanocomposite (TFN) Membranes

In general, thin film nanocomposite membranes consist of selective and support layers. In particular, the thin film nanocom-

posite membranes for water treatment are generally made of polyamide (PA) films and nanoparticles which are further supported by a heteromatrix such as polyvinylidene fluoride (PVDF). Thin film nanocomposite membranes are synthesized via interfacial polymerization (IP), a process that involves a polycondensation reaction at the interface of two mutually immiscible monomer solutions (Figure 4c). Livingston and co-workers showed the path to incorporate MOF particles as filler into thin

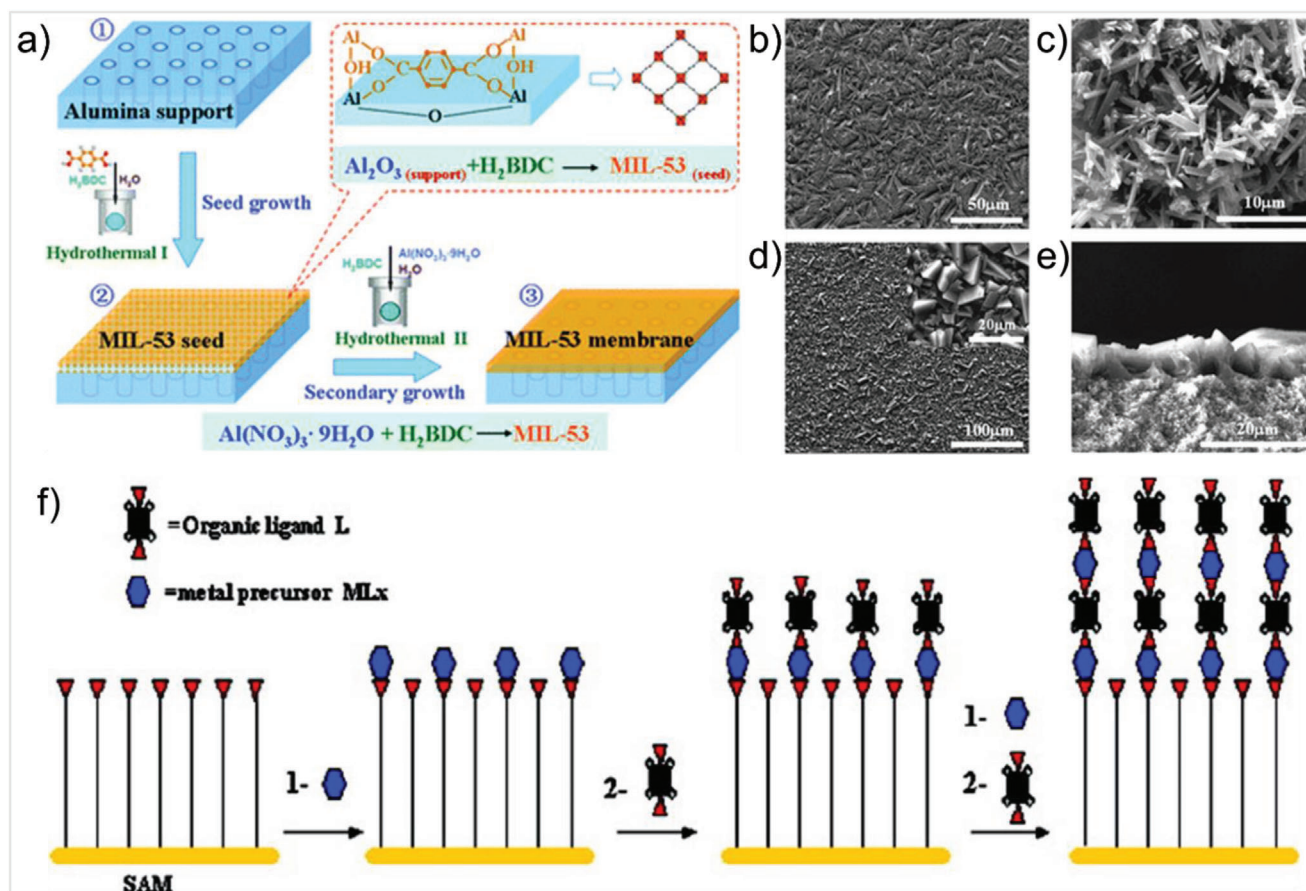


**Figure 5.** a) Schematic diagram of preparation of the MIL-53 membrane on alumina support via the reactive seeding method. SEM images of the b) MIL-53 seed layer, c) MIL-53 powders, d) MIL-53 membrane surface, and e) MIL-53 cross-section. Reproduced with permission.<sup>[142]</sup> Copyright 2011, The Royal Society of Chemistry. f) Schematic diagram for the step-by-step growth of the MOFs on the SAM by repeated immersion cycles, first in solution of metal precursor; and subsequently, in a solution of organic ligand. Reproduced with permission.<sup>[153]</sup> Copyright 2007, American Chemical Society.

film nanocomposite membranes (Figure 6a).<sup>[156]</sup> Owing to their ideal particle sizes, ordered porous structures, and pore sizes, MOFs-embedded thin film nanocomposite membranes showed better composite formation ability with the polymer matrixes than that of other nanoparticles.<sup>[149]</sup> A few examples of interfacial polymerization to fabricate MOF-based thin film nanocomposite membranes with enhanced overall performance are summarized here. In 2017, Chen and co-workers demonstrated the incorporation of UiO-66(Zr) nanoparticles into a polyamide active layer via an interfacial polymerization method to fabricate MOF-based thin film nanocomposites.<sup>[157]</sup> The thin film nanocomposite membrane exhibited enhanced permeability compared to the polymer membrane along with very good ion rejection and forward osmosis performance (Figure 6b). In another report, Ulbricht and co-workers established an efficient strategy to incorporate an Ag-based MOF into the nanoscale polyamide layer synthesized via interfacial polymerization of the polyethersulfone (PES) substrate to form a thin film nanocomposite membrane.<sup>[158]</sup> The MOF included thin film nanocomposite membrane found to exhibit improved hydrophilic surface along with lower transport resistance, while maintaining the membrane selectivity even at the low mass loadings of MOF with respect to the polymer. Moreover, the thin film nanocomposite membrane also showed enhanced

water flux and improved desalination performance during seawater desalination. In 2019, Li and co-workers established a strategy to introduce ZIF-8(Zn)-based hydrophilic hollow nanocubes into the polyamide layer via interfacial polymerization method to fabricate thin film nanocomposite membrane.<sup>[159]</sup> The H were synthesized via etching of ZIF-8(Zn) which yielded in HHNs with a higher number of hydroxyl groups on the surface and improved hydrophilicity of the material. The HHN-based thin film nanocomposites were found to exhibit excellent permeability (improved by 190%) and high ion rejection rates (improved by 2%) in comparison to the only thin film composite membrane. In another report, Wang, Huang, and co-workers demonstrated an approach to introduce three different water-stable MOFs (UiO-66-NH<sub>2</sub>(Zr), MIL-53(Al), and ZIF-8(Zn)) via blending and preloading interface polymerization method to fabricate thin film nanocomposite nanofiltration membranes.<sup>[160]</sup> The introduction of these MOFs was found to improve water permeability (by 30%) of thin film nanocomposite membranes while maintaining the rejection performance. The incorporation of various MOF nanoparticles via the interfacial polymerization method to synthesize thin film nanocomposite membranes certainly promises to produce next-generation membrane material. Hence, a better understanding of the role of MOFs along with other physical

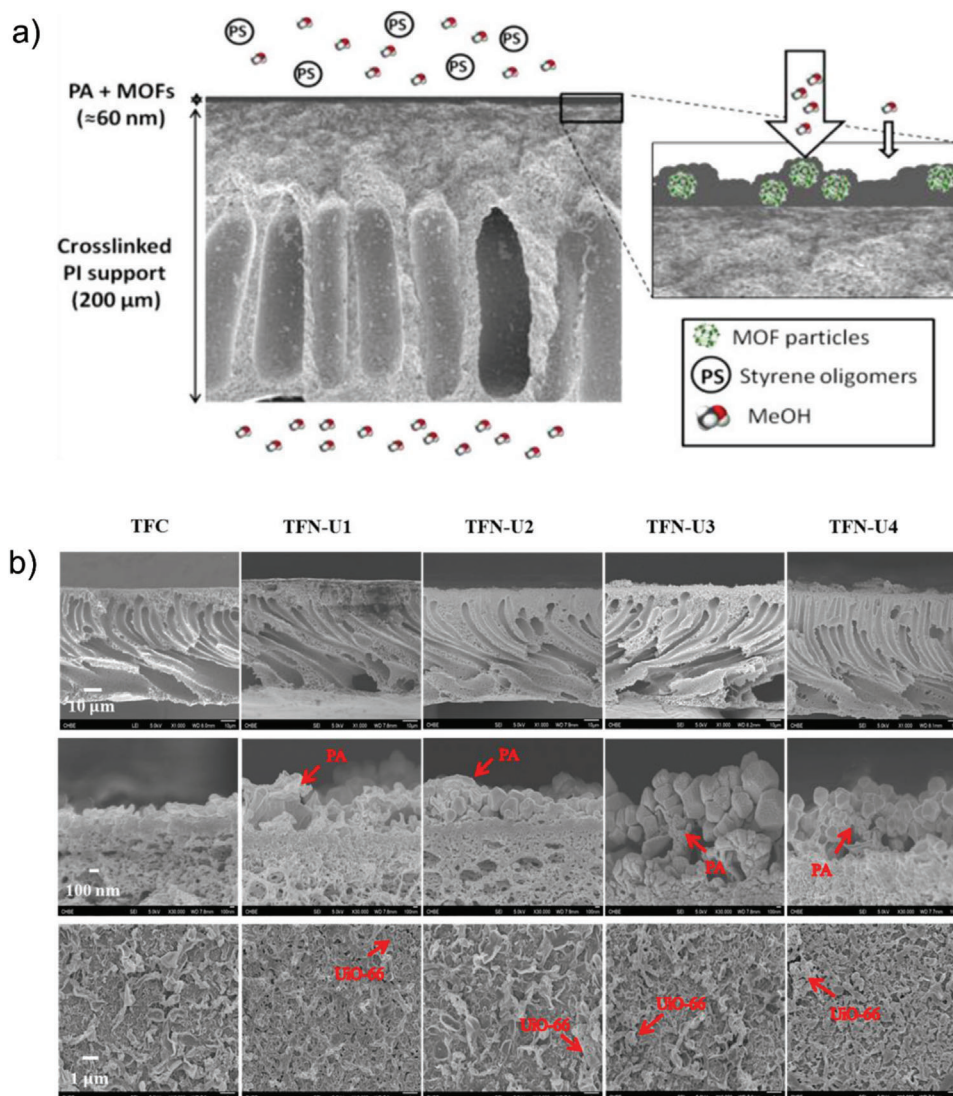


**Figure 6.** a) High flux MOF-based thin film nanocomposite membranes for Organic Solvent Nanofiltration. Reproduced with permission.<sup>[156]</sup> Copyright 2013, American Chemical Society. b) FESEM micrographs of cross-section and top surface for FC and thin film nanocomposite membranes with different UiO-66 loadings. Reproduced with permission.<sup>[157]</sup> Copyright 2017, American Chemical Society.

and chemical parameters can consolidate the molecular design and synthetic strategies of thin film nanocomposite membranes. Apart from interfacial synthesis, dispersing MOF precursors into two immiscible solutions to obtain MOF membranes is also being investigated to improve the membrane.<sup>[161]</sup>

The methods of incorporation of MOF particles during thin film nanocomposite membranes fabrication play an important role in the location and distribution in the selective layer. Moreover, it also affects the overall configuration, physiochemical properties, topology, and separation efficiency of the as synthesized membranes. Preparation of thin film nanocomposite membranes via interfacial polymerization has been done by pre-mixing MOF particles into the organic phase in which the MOF particles tend to be in the upper layer of the polyamide matrix. On the other hand, MOF particles dispersed in the aqueous phase tend to stay at the bottom layer. However, optimization of the loading amount of the MOF particles is one of the current scien-

tific interests to obtain optimal performance with reduced cost. In this regard, alternative methods such as in situ growth/assembly, spray-coating, spin-coating, filtration, and co-deposition can be utilized rather than the conventional method to fabricate thin film nanocomposite membranes. For example, in 2018, Navarro and co-workers demonstrated positioning of a monolayer of MIL-101(Cr) nanoparticles in thin film nanocomposite membrane in which a Langmuir–Schaefer MOF-film was introduced between the P84 substrate and the thin polyamide layer. This method was found to be involved with very small amount of MOF loading (i.e.,  $3.8 \mu\text{g cm}^{-2}$ ).<sup>[216]</sup>

Spin-coating has been regarded as another efficient method to deposit thin films on any flat substrates with better uniformity by virtue of its centrifugal forces. Typically, this method involves loading of suspended MOF particles onto the center of the substrate and a high-speed controllable centrifugal force outspreads the suspended solution as a thin film. This method offers high

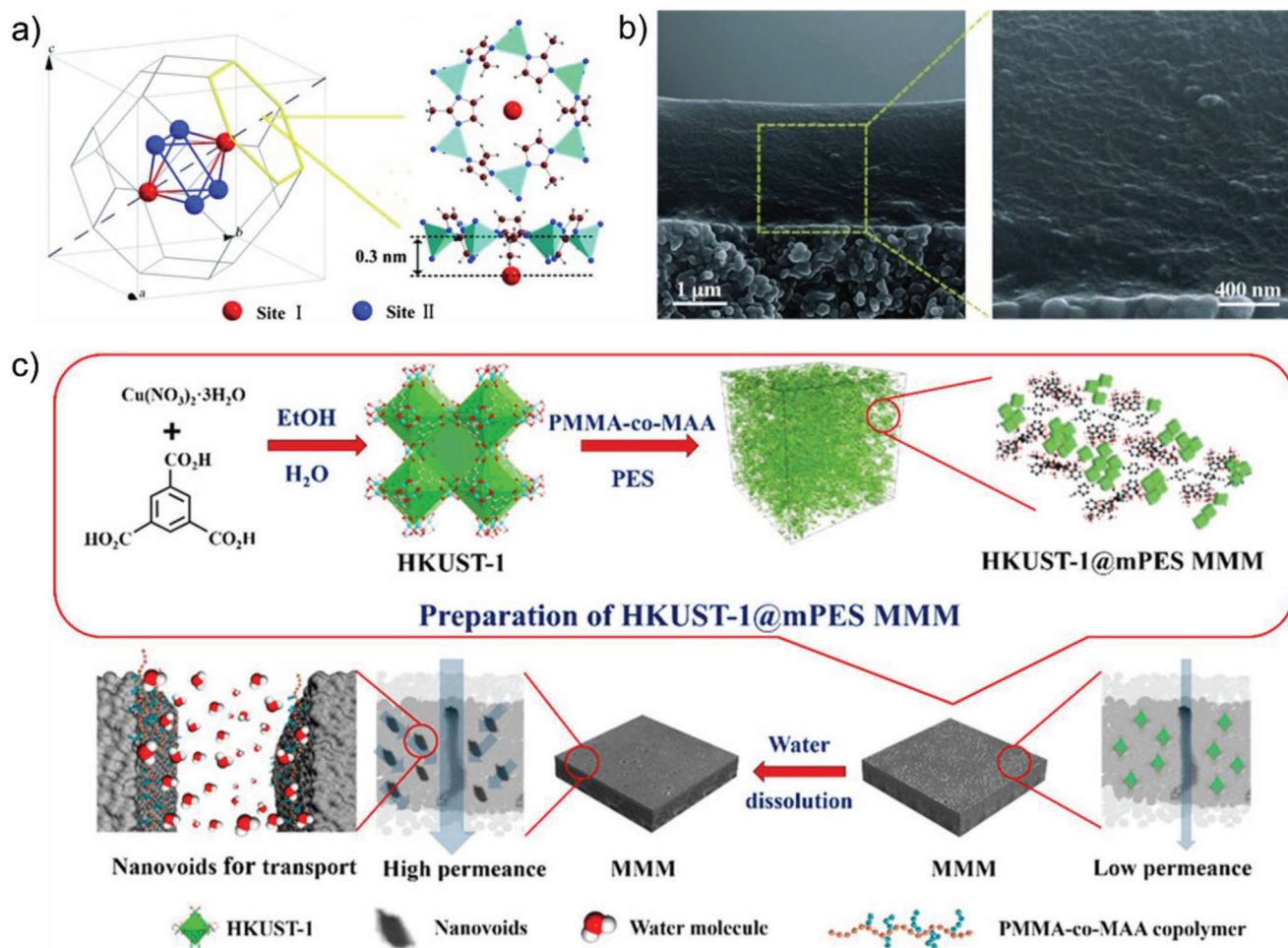


**Figure 7.** a) Representations of isobutanol adsorption sites in ZIF-8(Zn). b) Cross-sectional SEM images of the ZIF-8(Zn)-PMPS membrane. Reproduced with permission.<sup>[163]</sup> Copyright 2011, Wiley-VCH. c) Schematic illustration of HKUST-1(Cu)@mPES MMM prepared by the nanovoid-generated approach and its application for highly efficient water treatment. Reproduced with permission.<sup>[165]</sup> Copyright 2019, American Chemical Society.

degree of controllability as the properties of the thin film such as thickness can also be tuned by controlling the spin velocity, viscosity of the coating solution, and the solvent evaporation rate. In addition, MOF particles can also be incorporated into thin film nanocomposite membranes during interfacial polymerization through the organic solutions. However, the MOF particles can get agglomerated in the organic phase particularly at the relatively higher loading and tend to stay at the selective layer, resulting in deformities inside the membrane structure. In this regard, surface engineering of MOF particles with proper functional groups can be helpful to improve their dispersity in the oil phase. Moreover, attention should also be given to prevent the sedimentation of MOF particles during the fabrication of thin film nanocomposite membranes which can eventually reduce the particle agglomeration.

### 6.2.2. Mixed Matrix Membrane

The mixed matrix membranes are typically composite membranes fabricated from a combination of inorganic/inorganic-

organic hybrid materials acting as the additive or filler and a polymer matrix serving as the continuous phase (Figure 4d). In the case of MOF-based MMMs, the MOF particles are introduced as the filler in the membrane.<sup>[149,162]</sup> Recent years have witnessed a drastic upsurge in the development of MOF-based MMMs owing to their less cost, relatively easy scale-up, and greater stability than other membranes. The blending method is the most utilized strategy to obtain MOF-based MMMs,<sup>[162]</sup> and depending upon the substrate utilization, it can be divided into: blending with substrate or without substrate. The blending with substrate process generally consists of three consecutive steps: 1) mixing the MOF and polymer into the solvent; 2) introduction of mixed solution in porous supports via dip-coating, spin-coating, and so on, and 3) removal of casting solvent.<sup>[149]</sup> For example, Li, Wang, and co-workers synthesized a MOF based MMM, namely ZIF-8(Zn)/PMPS MMM by introducing the solution of ZIF-8(Zn) nanoparticles and polymethylphenylsiloxane (PMPS) in alumina capillary tubes as supports. The ZIF-8/PMPS MMM was found to exhibit very high isobutanol permeability performance (Figure 7a,b).<sup>[163]</sup> In another report, Tang and co-workers demonstrated incorporation of MOFs particles into

chitosan polymeric matrix to fabricate a positively charged nanofiltration membrane.<sup>[164]</sup> NH<sub>2</sub>-MIL-101(Cr) and NH<sub>2</sub>-MIL-101(Al) were homogeneously dispersed in the chitosan polymeric matrix which resulted in enhanced salt-rejection performance and removal efficiency toward multivalent cations. In 2019, Matsuyama and co-workers established a new class of MOF-based MMM, namely HKUST-1(Cu)@mPES MMMs via a nanovoid-generated approach based on the blending method (Figure 7c).<sup>[165]</sup> In 2021, Xie and co-workers reported a hydrophilic/hydrophobic dual-layer membrane fabricated from an aluminum fumarate MOF-doped poly(vinyl alcohol) based dense layer as the top layer and a hydrophobic microporous polytetrafluoroethylene as the substrate layer.<sup>[166]</sup> In this work, the authors demonstrated the role of appropriate MOF loading within the mixed matrix hydrophilic layer toward simultaneous enhancement of water vapor flux and wetting resistance of the material. Moreover, the dual-layer membrane was also found to exhibit long term stability toward real seawater systems. Apart from membrane desalination processes, MMMs can be very much useful in case of pervaporation or thermal desalination. In 2016, Chung and co-workers demonstrated molecular engineering of MOF with alumina surface to obtain nature-mimetic hydrophobic MOF-based mixed matrix membranes with high wetting resistance for seawater desalination via vacuum membrane distillation.<sup>[167]</sup> Such synthetic strategy assisted in inclusion of advantages of both alumina supports (high water permeability and high stability) and MOF matrix (hydrophobic surface). In 2019, Zhao and co-workers reported a series of mixed matrix membranes with defect-free active layer around 1 μm thickness for ethanol permselective pervaporation.<sup>[168]</sup>

### 6.3. Other MOF-Based Membranes

Apart from the common synthetic methods for composite membrane synthesis discussed above, researchers have explored the possibilities of developing more cost and energy-efficient synthetic strategies such as electrospinning, pressure-assisted self-assembly (PASA), fine-tuning contra-diffusion, phase transformation interfacial growth (PTIG), solvent-free hot-pressing, and gel-vapor deposition (GVD). Electrospinning is a comparatively recent technique to produce polymer membranes fabricated with micron or submicron level microfibers.<sup>[169]</sup> The electrospinning has been the popular choice method to synthesize polymer composite membranes owing to its advantages such as continuous nanofabrication, scalability and low cost.<sup>[170]</sup> In this line, Efome and co-workers in their recent study demonstrated loading of an Fe-MOF up to 5 wt% into PVDF matrix via electrospinning to fabricate superhydrophobic nanofibrous membrane.<sup>[171]</sup> The inclusion of MOF particles contributed to the enhancement of the porous characteristics as well as the fiber diameter of the membrane which was found to be beneficial for its excellent direct contact membrane distillation and salt rejection performance. The pressure-assisted self-assembly technique was designed in such a way that it could easily deposit the flexible and packed layers of the filler materials onto the substrates. In 2013, Hung and co-workers showed strategic utilization of the pressure-assisted self-assembly technique to execute controlled sequencing of the graphene oxide (GO) flexible layers on the

polyacrylonitrile support.<sup>[172]</sup> The deposition of GO was established to not only maintain the permeation flux but also to enhance the pervaporation separation performance of the membrane. Next to this, the fine-tuning contra-diffusion technique offered permeation flux and control over mass transfer resistance via contra-diffusion.<sup>[149,173]</sup> In an early report by Yao, Wang and co-workers demonstrated the first example of the fabrication of ZIF-8(Zn) films on a polymer substrate via the contra-diffusion technique.<sup>[173]</sup> The contra-diffusion method was found to be beneficial not only for the facial and direct growth of MOF particles on the polymer substrates but also to impart significant control over the microstructure and thickness of the films/membranes, which could be tuned for different applications. In 2018, Li, Wang, and co-workers developed a new technique, namely phase transformation interfacial growth, which enables formation of a defect-free MOF layer via single-step interface growth.<sup>[161a]</sup> This strategy turned out to be extremely efficient for polymeric substrate formation and the growth of the MOF layer. In 2016, Wang and co-workers established a novel solvent- and binder-free method to fabricate stable MOF membranes called the hot-pressing (HoP) method.<sup>[174]</sup> In this method, formation of the MOF layer on the substrate occurs as the first step, followed by uniform distribution of the MOF layer via the HoP method. This method was found to enhance the robustness of the MOF coating while maintaining the crystallinity of the MOFs. Advancing this technique, another novel method, namely roll-to-roll processing, has been developed. Roll-to-roll processing method offers effective mass production of MOF coating and better control over total mass loading of MOFs and their particle size.<sup>[175]</sup> In 2017, Li and co-workers demonstrated a unique approach to fabricate ultrathin MOF-membrane, termed as gel-vapor deposition method.<sup>[176]</sup> The gel-vapor deposition method offers several advantages such as solvent free synthesis, low cost, shorter synthesis time, and scalability. Moreover, it enables the in situ formation of MOF membranes on a small scale with large effective membrane areas and allows the formation of MOF membranes having different topologies on the substrates. In addition, this method imparts control over mass transport along with fluid dynamics of reactants and heterogeneous crystallization, affording an alternative scalable method for ultrathin MOF-based membranes production of water treatment applications.

## 7. Recent Progress of MOFs-Based Materials for Desalination

In the recent progress of MOFs and MOF-membranes with respect to capacitive deionization, forward osmosis, adsorption desalination, reverse osmosis, membrane distillation, nanofiltration, ultrafiltration, microfiltration, and other methods will be discussed (Table 3).

### 7.1. Capacitive Deionization

Capacitive deionization was first rationalized in the 1960s and has attracted much scientific as well as industrial attention over the last few decades as an emerging alternative solution for water desalination.<sup>[177]</sup> Typically, in capacitive deionization I technology, the salts of the feed solution get temporarily stored in an interfacial double layer between the salt solution and the capacitive



**Table 3.** Summary of key examples of MOF-based desalination.

Process	Type of membrane	MOF	Method	Membrane thickness	Pressure [bar]	Permeability (L m <sup>-2</sup> h <sup>-1</sup> bar <sup>-1</sup> )	Salts	Concentration [ppm]	Rejection [%]	Ref.
RO	Free standing membrane	ZIF-8	Solvothermal	29.43 Å	60	NA	NaCl	0.5 M	99	[202]
RO	Grown on alumina support	UiO-66	In situ solvothermal	2.0 µm	10	0.28	Mixed of saline water	2000	98	[197]
RO	TFN (PA)	ZIF-8	IP	100 nm	15.5	3.35	NaCl	2000	98.5	[204]
RO	TFN (PA)	ZIF-8	IP	150 µm	15	1.68	NaCl	2000	99.4	[206]
RO	TFN (PA)	MIL-101 (Cr)	IP	100–300 µm	16	2.2	NaCl	2000	99	[221]
RO	TFN (PA)	MIL-125	IP	NA	20.6	3.64	NaCl	2000	98.4	[222]
RO	TFN (PA)	UiO-66	IP	NA	20.6	4.13	NaCl	2000	98.6	[222]
RO	TFN (PA)	PCN-222 treated myristic acid	IP	300 nm	17.6	5.8	NaCl	2000	96	[208]
RO	TFN (substrate)	HKUST treated sulfuric acid	IP	0.029 µm	15.5	3.03	NaCl	2000	96	[209]
RO	TFN (PA)	ZIF-8	IP	250 nm	15.5	3.95	NaCl	2000	99.2	[205]
FO	TFN (PA)	UiO-66	IP (blending)	200 nm	NA	3.33	NaCl	2000	95.3	[195]
FO	TFN (PA)	Silver based MOFs	IP (blending)	100 nm	NA	~5	NaCl	2000	97	[158]
FO	TFN (PA)	CuBDC-NS	IP (blending)	30-40 nm	NA	1.13	NaCl	1000	97.6	[196]
FO	TFN (PA)	PSS-coated ZIF-8 treated TEA	IP	250 nm	NA	5.688	NaCl	Synthetic seawater	90	[197]
NF	TFN (PA)	UiO-66	IP	50–100 nm	10	11.5	NaCl	1000	38	[223]
							MgCl	1000	90	
							MgSO <sub>4</sub>	1000	90	
							Na <sub>2</sub> SO <sub>4</sub>	1000	93	
NF	TFN (PA)	UiO-66-NH <sub>2</sub> treated palmitoyl chloride	IP	380 nm	4	12.4	NaCl	1000	28	[215]
							MgSO <sub>4</sub>	1000	92	
							Na <sub>2</sub> SO <sub>4</sub>	1000	98	
NF	Grown on PDA modified alpha Al <sub>2</sub> O <sub>3</sub> disc	ZIF-8	In situ solvothermal	20 µm	NA	30.8	Seawater	~35000	99.8	[224]
NF	Vacuum filtration of UiO-66-NH <sub>2</sub> in PIP solution	UiO-66-NH <sub>2</sub>	Solvothermal	93 nm	6	31	NaCl	1000	21.3	[158]
							MgCl	1000	58	
							MgSO <sub>4</sub>	1000	91.2	
							Na <sub>2</sub> SO <sub>4</sub>	1000	97.3	
NF	TFN (substrate)	CuBTC	Blending in substrate	100	8	6.91	NaCl	1000	44.9	[225]

(Continued)

Table 3. (Continued).

Process	Type of membrane	MOF	Method	Membrane thickness	Pressure [bar]	Permeability (L m <sup>-2</sup> h <sup>-1</sup> bar <sup>-1</sup> )	Salts	Concentration [ppm]	Rejection [%]	Ref.
NF	TFN (PA)	MIL-53 (Al)	IP (blending)	200	10	6.91	MgSO <sub>4</sub>	—	97.3	—
—	—	—	IP (pre-loading)	—	—	6.69	NaCl	10 mmol	40.4	[160]
NF	TFN (PA)	UiO-66-NH <sub>2</sub>	IP (blending)	200	10	7.19	NaCl	10 mmol	34.6	—
—	—	—	IP (pre-loading)	—	—	6.97	—	—	42.1	[160]
NF	TFN (PA)	ZIF-8	IP (blending)	200	10	7.13	NaCl	10 mmol	36.1	—
—	—	—	IP (pre-loading)	—	—	7.36	—	—	35.4	[160]
MD	Grown on alumina substrate	NH <sub>2</sub> -MIL-53(Al)	Solvothermal	NA	0.02	32.2	NaCl	35000	33.8	—
—	—	—	—	—	—	—	—	—	≈99	[167]
MD	Nanofibrous blended polymer membrane	Fe-BTC	Blending in polymer solution	0.8	2.87	NA	NaCl	35000	≈99	[171]
MD	Coating layer of substrate	ZIF8/Chitosan	Dip coating	100 nm	1.25	8.05	NaCl	35000	99.5	[213]

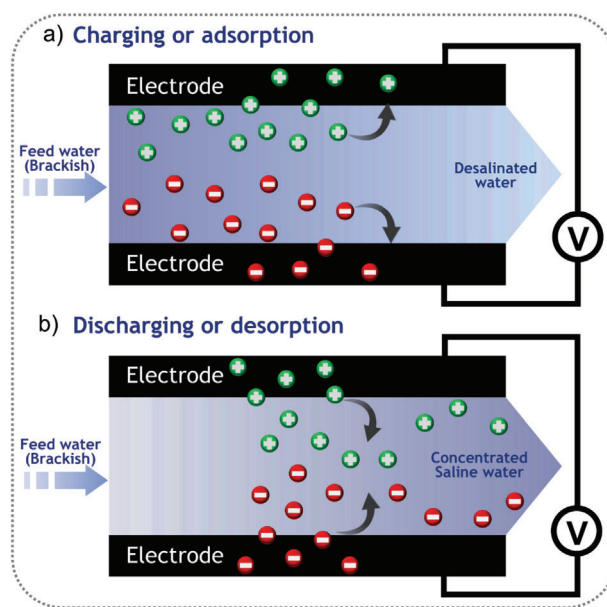
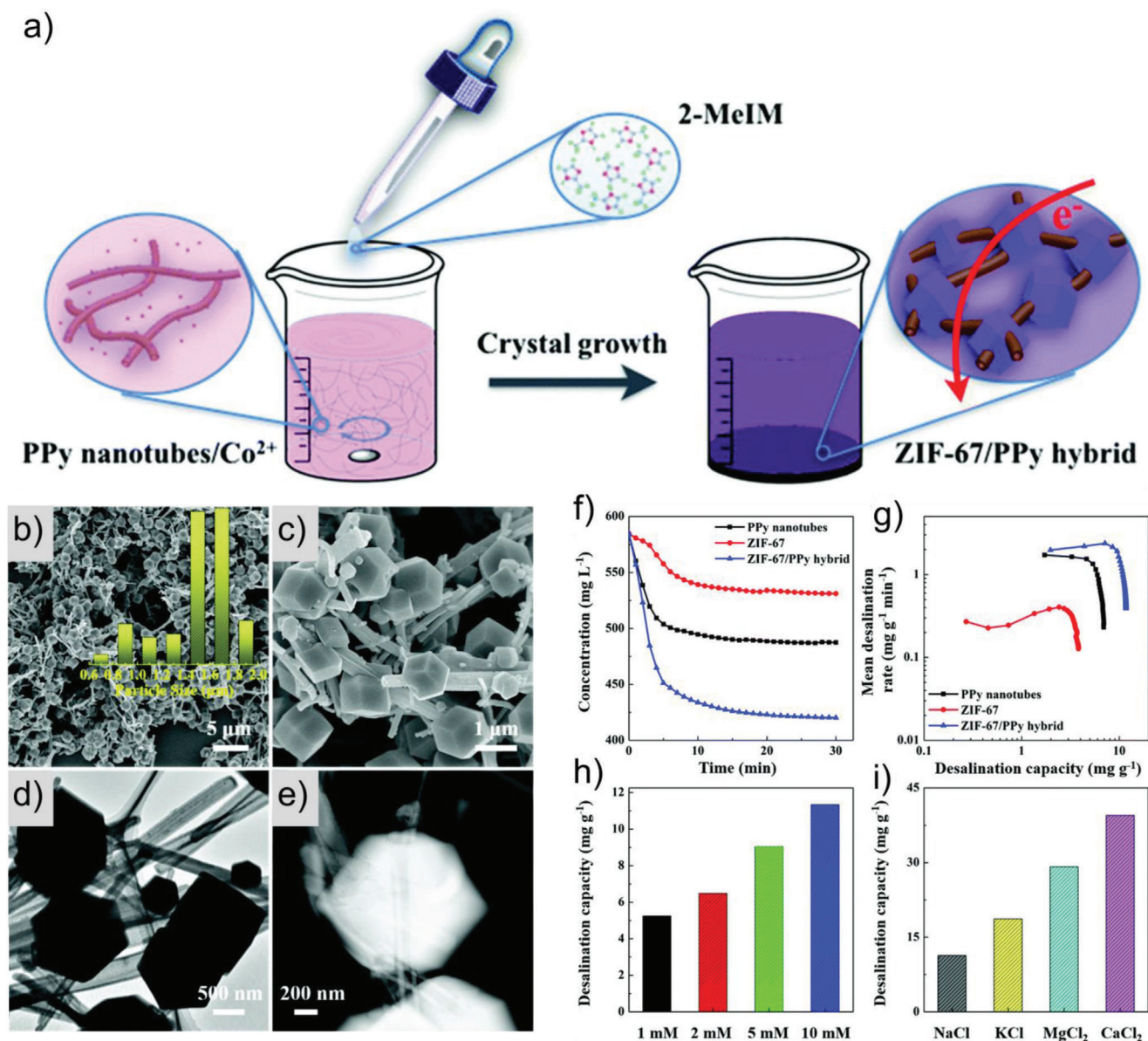


Figure 8. a) Deionization of saline water and b) regeneration of capacitive deionization electrodes.

deionization electrode (Figure 8). In comparison with other techniques, capacitive deionization offers several advantages such as environmentally friendly operation, no chemical additives, and low energy footprints (even lower than electrolysis potential of water [ $\approx 1.23$  V]).<sup>[178]</sup> The capacitive deionization process involves both deionization and capacitive processes in which electrostatic forces are applied via oppositely charged electrodes to remove the ions from saline water. Further, the saturated electrodes can also be regenerated by transferring the adsorbed ions into wash water via reverse potential gradient between the respective electrodes.<sup>[179]</sup> Development and improvement of the electrode properties are quintessential for the capacitive deionization process; in particular, high electrochemical stability, high electronic conductivity, and high surface area for accessing larger ions, resulting in an enhanced capacitive deionization performance.<sup>[177]</sup> Hence, efforts are being made to develop and test new materials for the membrane capacitive deionization process. Although various porous carbons, such as activated carbon, carbon nanofiber, carbon nanotubes, mesoporous carbon, reduced graphene oxide, and carbon nanospheres have been employed as electrode material for the capacitive deionization process, they often get oxidized easily, which particularly limits their long-run applicability and large-scale use.<sup>[180–187]</sup> To address this problem, Xu, Yang, and Yamauchi and co-workers demonstrated the first example of using MOFs as the active material for capacitive deionization without any further carbonization.<sup>[188]</sup> ZIF-67(Co) was incorporated into polypyrrole nanotubes via an in situ method, which resulted in a 3D hybrid material having the ZIF-67(Co) particles interconnected through the nanotubes and enabled electron transfer. The hybrid electrode material was found to have merits from both ZIF-67(Co) (regular micropores and high porosity) and polypyrrole nanotubes (high electrical conductivity) (Figure 9). Such fascinating combined properties resulted in an excellent desalination capacity of 11.34 mg·g<sup>-1</sup> along with excellent recyclability.



**Figure 9.** a) Scheme illustrating the synthetic procedure of a ZIF-67/PPy hybrid. b,c) FESEM, d) TEM, and e) HAADF-STEM images of the ZIF-67/ PPy hybrid. f) Salt concentration variations and g) capacitive deionization Ragone plots of the PPy nanotubes, ZIF-67, and ZIF-67/PPy hybrid. Capacitive deionization performances of the ZIF-67/PPy hybrid h) at various NaCl concentrations and i) in various metal ion solutions (10 mM). Reproduced with permission.<sup>[188]</sup> Copyright 2019, The Royal Society of Chemistry.

Another report by Yang and co-workers has shown the utilization of a series of bimetal MOFs (BMOFs) with different Co/Zn molar ratios for superior membrane-based capacitive deionization performance.<sup>[189]</sup> Further, most of the metallic species were removed from the pristine MOFs through in situ pyrolysis and chemical etching process to obtain MOF-derived graphitized carbons. It was observed that the molar ratio of Zn/Co ions played a crucial role in determining the specific surface area and graphitization degree. The best performing porous carbon obtained from the BMOF (Zn:Co = 3:1) showed a salt removal capacity of 45.62 mg g<sup>-1</sup> at 1.4 V and a very high-performance retention ability.

## 7.2. Forward Osmosis

Forward osmosis process has been considered the most efficient desalination method owing to its operational low energy footprints.<sup>[190]</sup> The forward osmosis process operates via two steps: first, osmotic dilution of the draw solution and second, the permeation of pure water from the modified draw solution.<sup>[191]</sup> The main advantage of forward osmosis-based membranes over other membranes relies on their energy-efficient working principle as it operates at low or no hydraulic pressures. In general, the process is based on osmosis-driven solute movement acting as the driving force in the diffusion of solute with a

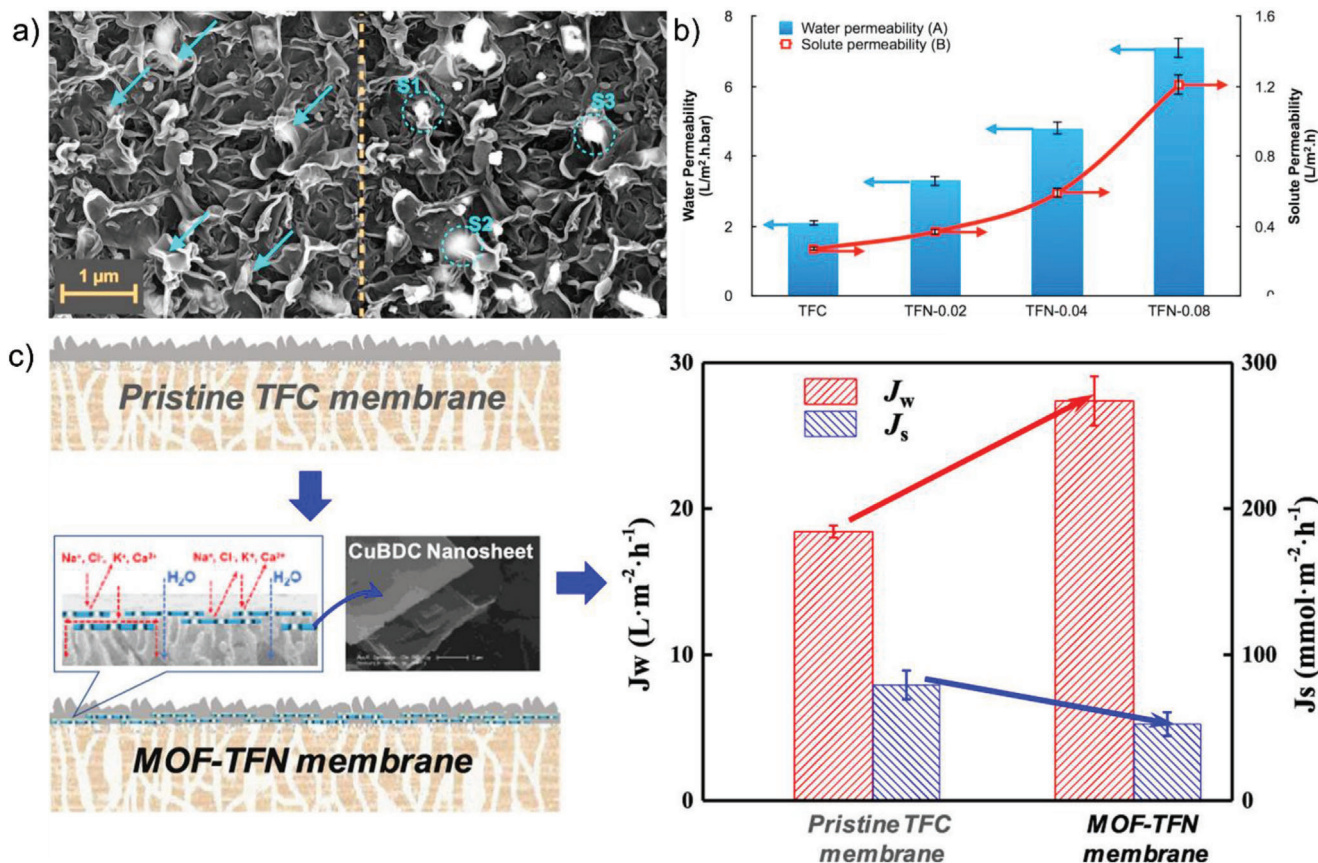


**Figure 10.** a) FE-SEM image of the thin film nanocomposite-0.08 membrane using the secondary (left-side) and the backscattered (right-side) electron imaging detector. b) Transport parameters of the membranes including water (A) and solute (B) permeability; Reproduced with permission.<sup>[158]</sup> Copyright 2017, Elsevier. c) MOF nanosheet incorporated thin-film nanocomposite membrane for high-performance forward osmosis. Reproduced with permission.<sup>[196]</sup> Copyright 2019, Elsevier.

lower concentration to solute with a higher concentration. In this method, the osmotic pressure necessary to draw fresh water out of the feed solution is created by the draw agents.<sup>[192]</sup> Typically in desalination, seawater or brackish water is used as feed solution having lower concentration than the draw solution and a semi-permeable membrane will be placed between them. Further, because of the difference in chemical potential, water from the saline solution will transport to the draw solution chamber through the semi-permeable membrane. Subsequently, water is extracted from the draw solution via membrane distillation or employing moderate heat and the draw solution will be recycled for several cycles. In this regard, introduction of MOF particles as an additive in forward osmosis membranes has proven to be beneficial in improving the water flux, salt rejection, and reverse solute flux of the membrane. To fabricate forward osmosis membranes, two main prerequisites have been considered: 1) thin film composite membranes with ultra-slim active layers over the permeable support layer and 2) robust outer surface asymmetrical membranes with coordination between the permeable layer and the surface layer.<sup>[193,194]</sup> However, utilization of MOF-integrated membranes for desalination via the forward osmosis process is still limited and MOF-incorporated thin film composite membranes are found to be the choice of material for this purpose. In 2017, Han, Chen and co-workers fabricated a new thin film

nanocomposite membrane with superhydrophilic UiO-66(Zr) nanoparticles which were found to affect the surface morphology, hydrophilicity, and selective layer chemistry significantly.<sup>[195]</sup> The UiO-66(Zr) incorporated thin film nanocomposite exhibited improved water permeability along with almost unaltered rejection performance and enhanced forward osmosis performances. The best performing membrane, that is, TFN-U2 with 0.1 wt% MOF loading showed 52% improvement in water permeability and a 25% increase in water flux. In another work, Ulbricht and co-workers have reported incorporation of Ag-based MOF nanocrystals into nanoscale polyamide layer via interfacial polymerization to fabricate thin film nanocomposite membrane.<sup>[158]</sup> The incorporation of MOF nanocrystals induced several advantages such as improved hydrophilic surface owing to the presence of carboxylic acid functionalities of the MOFs along with lower transport resistance for the selective layer of the membrane (Figure 10a). Particularly, very low MOF loading (0.04%) was found to enhance the pure water permeability of the membranes up to 129% (Figure 10b). Owing to such combined advantages, the modified membrane showed excellent performance toward seawater desalination forward osmosis process and higher water flux (34 L m<sup>-2</sup> h<sup>-1</sup>) with real seawater samples. In 2019, Wang and co-workers have demonstrated incorporation of a 2D MOF as the nanofiller in the active layer to fabricate composite

thin film nanocomposite membrane with enhanced water permeability and forward osmosis performances (Figure 10c).<sup>[196]</sup> The MOF nanosheet, namely CuBDC-NS, was incorporated into polyamide active via interfacial polymerization. The thin film nanocomposite membrane with 0.12 wt/v% CuBDC-NS was found to increase the forward osmosis water flux by as high as 50% along with the reduction in specific reverse solute flux also by 50%. In addition, the thin film nanocomposite membrane exhibited improved performance in the continuous flow experiments with real wastewater in comparison with the pristine components. Moreover, improvement in the antifouling capability of the thin film nanocomposite membrane resulted in enhanced hydrophilicity and biocidal activity. In an interesting work by Ooi and co-workers, ZIF-8(Zn) nanoparticles were coated with poly(sodium-4-styrenesulfonate) (PSS) to fabricate a thin film nanocomposite membrane with enhanced swelling resistance and water permeability.<sup>[197]</sup> This anionic nature of the polymer contributed to improving the hydrolytic stability of ZIF-8(Zn) nanocrystals via intermolecular electrostatic stabilization. The PSS-coated ZIF-8(Zn) thin film nanocomposite membrane showed improved pure water permeability of 116.2% along with a very good NaCl rejection rate in comparison to the thin film nanocomposite membrane without TEA. In addition, the thin film nanocomposite membrane exhibited very good swelling resistance against both oil emulsion and water, which is correlated to the charged nature of ZIF-8(Zn) and rigidification of polyamide matrix by MOF particles, respectively.

### 7.3. Adsorption Desalination

Adsorption desalination emerged as an alternative technique for water desalination owing to its low-cost, energy-efficient operation, and environmentally friendly properties. Adsorption desalination technology is based on multiple consecutive processes: evaporation followed by adsorption/desorption and subsequent condensation. In the first cycle, the feed water allows to evaporate via a low-pressure evaporator which subsequently gets adsorbed by an adsorbent material. These adsorbent materials generally remain as two or more sorbent beds enabled with a heat exchanger. Once the first step is completed, the sorbents beds are heated with hot water through the heat-exchanger tubes and the vapor gets released. Further, the vapor is collected through a condenser by employing cool water.<sup>[198]</sup> Although the most common adsorption desalination setup involves utilization of silica gel as the bed material, it suffers from major limitations such as the lack of hydrophilicity, which eventually results in low adsorption capacity and average performance. In this regard, the utilization of hydrophilic nanocrystals of porous MOFs is believed to be the most efficient solution to address this issue. In 2016, Elsayed and co-workers investigated the role of MOFs as adsorbents for beds.<sup>[199]</sup> For this study, the authors chose three MOFs, namely Al-Fumarate, MIL-101(Cr), and CPO-27(Ni) with diverse structural and physicochemical properties. The experimental and simulation results showed CPO-27(Ni) is well suited for conditions having low evaporation temperature (5 °C) and high regeneration temperature ( $\geq 110$  °C). The Al-Fumarate worked well at high evaporator temperatures (20 °C), whereas MIL-101(Cr) was found to outperform all the other adsorbent materials at that

time. In this context, to understand the adsorbate–adsorbate and adsorbent–adsorbate interactions, Kim et al. examined the adsorption/desorption enthalpy of zeolite (13X and MgY24) and MOF-801(Zr) with water as an adsorbate. Results indicated that MOF-801(Zr) possesses lesser adsorption enthalpy compared to type I zeolites. Such an in-depth understanding of thermodynamics can help in designing efficient sorbent material for AD.<sup>[200]</sup>

### 7.4. Reverse Osmosis

Reverse osmosis is the most commonly adapted and large-scale employed desalination process with more than 20 000 installed reverse osmosis plants globally. In the reverse osmosis method, the water molecules from higher solute concentrations are transported to the low solute concentration upon applying external pressure which acts as the driving force to pass the water molecules through the membrane. Owing to its large-scale global utilization, many efforts have been devoted to address and improve the trade-offs between kinetics and energetics associated with this process.<sup>[201]</sup> To this end, during the last decade, MOFs have shown good promise as the fillers of polymeric membranes to counter the limitations of the state-of-the-art. In 2011, Jiang and co-workers have conceptualized the idea of utilization of MOFs embedded membrane for reverse osmosis-based desalination process.<sup>[202]</sup> The authors have presented a proof-of-concept theoretical simulation to evaluate the potential of the ZIF-8(Zn) membrane toward the desalination process where the ZIF-8(Zn) membrane was subjected to an aqueous solution of NaCl having almost seawater concentration. The simulation results revealed that it can perform desalination under external pressure and both anions and cations cannot penetrate the membrane which can be attributed to the sieving effect imparted due to the small pore apertures of ZIF-8(Zn). In 2015, the same research group reported another simulation study where five different types of ZIF membranes, namely ZIF-25, -71, -93, -96, and -97 were examined for water desalination performance.<sup>[203]</sup> The ZIF-based membranes were constituted of different imidazolate ligands having different functionalities in the ZIF-membranes along with different polarity and pore apertures. The simulation results indicated that ZIF-71, -25, and -96 possess higher water flux than that of ZIF-97 and -93 whereas the trend of affinity for water was found to be ZIF-96 > -71 > -25. In addition, all the ZIF-membranes showed good desalination potential. In the same year, Pinnau and co-workers demonstrated the incorporation of hydrophobic ZIF-8(Zn) nanocrystals into selective polyamide layer toward water desalination.<sup>[204]</sup> The incorporation of ZIF-8(Zn) nanocrystals rendered several advantages over the traditional zeolites such as better compatibility with the selective layer and faster water transport through the framework. Desalination results revealed that even lower loading of the MOF (0.05 wt%) can improve the water permeability by as high as 88%. Further, incremental loading of ZIF-8(Zn) resulted in enhanced water permeability by 162% in comparison with pure PA. In addition, the MOF membrane exhibited unaltered water permeability with brackish water filtration along with a high ion rejection of 98%. In another work, Park and co-workers studied the effect of different size of ZIF-8(Zn)

nanoparticles (60, 150, 250 nm) on the reverse osmosis performance of thin film nanocomposite membranes.<sup>[205]</sup> The nanoparticles deposition on the support layer was affected by their different size and the interfacial area between ZIF-8(Zn) and polyamide matrix was found to influence the reverse osmosis performance of the thin film nanocomposite membrane. Hence, the size of fillers can play a crucial role in interfacial polymerization as well as the reverse osmosis performance of the thin film nanocomposite membranes. In this line, Aljundi et. al. investigated the effect of the incorporation of ZIF-8(Zn) into the membrane on its fouling resistance.<sup>[206]</sup> A fouling study with bovine serum albumin as a model foulant revealed reduced fouling tendency of the membrane upon addition of ZIF-8(Zn) particles, improving the anti-fouling properties of the reverse osmosis membrane. Apart from ZIF-8(Zn), other chemically stable MOFs such as UiO-66(Zr) have been employed for the reverse osmosis process. In an interesting work, Li and co-workers reported the first example of UiO-66(Zr)-based membrane supported upon hollow alumina fibers fabricated via in-situ solvothermal synthesis (Figure 11a).<sup>[124]</sup> The fabricated composite membrane was found to exhibit excellent ion rejection performance of 86.3%, 98.0%, and 99.3% for  $\text{Ca}^{2+}$ ,  $\text{Mg}^{2+}$ , and  $\text{Al}^{3+}$ , respectively (Figure 11b). The ion rejection process was believed to be driven via size-exclusion mechanisms. In addition, the membrane showed good permeability ( $0.28 \text{ L m}^{-2} \text{ h}^{-1} \text{ bar}^{-1} \mu\text{m}$ ) and moderate permeance ( $0.14 \text{ L m}^{-2} \text{ h}^{-1} \text{ bar}^{-1}$ ) toward water desalination. These studies highlighted the significant role of small pore apertures of ZIF-8 and UiO-66 toward high salt rejection performance. In addition, the incorporation of MOF nanoparticles was found to improve the water permeability of the MOFs-integrated membranes owing to the hydrophilic functional groups which allowed more water flux with the faster movement of water through the porous substrate and thin film layer.<sup>[106]</sup> In 2016, Gao and co-workers reported doping of MIL-101(Cr) into a dense polyamide layer on the polysulfone support to fabricate a new thin film nanocomposite membrane for water desalination.<sup>[207]</sup> The porous framework of MIL-101(Cr) favored the establishment of direct water channels in the polyamide layer, which resulted in improved water permeance. Further, the thin film nanocomposite membrane showed very high NaCl rejection performance (>99%) even with very low MOF loading (0.05%). Martin, Morris and co-workers have exploited post-synthetic modification (PSM) as an efficient tool to functionalize the meso porous environment of a Zr-based MOF, namely PCN 222, to fabricate reverse osmosis membrane (Figure 11c,d).<sup>[208]</sup> Due to the mesoporous nature of the MOF, despite of the high-water flux in desalination process, the salt rejection performance was found to be poor. This problem was tactically addressed via performing PSM to attach myristic acid to the MOF nodes, which resulted in altered pore size distribution and channel dimensions. Further, a thin film nanocomposite membrane was fabricated utilizing the modified PCN 222 nanoparticles. Upon PSM with myristic acid, the thin film nanocomposite membrane was found to exhibit  $\approx 100\%$  of water flux along with high salt rejection performance (>95%) (Figure 11e,f). In 2017, Lee and co-workers reported the utilization of HKUST-1(Cu) in the support layer to fabricate a thin film composite membrane for reverse osmosis process.<sup>[209]</sup> HKUST-1(Cu) was treated with sulfuric acid, which imparted higher hydrolytic stability along with higher hydrophilicity and improved dispersivity

of the MOF particles within the polysulfone membrane. In addition, the acidified MOF particles enhanced the water permeability of the membrane. Further, the water flux was found to increase by 33% in comparison with pure reverse osmosis membranes while maintaining the salt rejection performance. In 2019, Wang and co-workers established a new class of hollow fiber-based thin film nanocomposite membranes with polydopamine modified HKUST-1(Cu) for low-pressure reverse osmosis of brackish water.<sup>[210]</sup> The MOF particles were incorporated in the polyamide support matrix with polyethersulfone substrate via the interfacial polymerization method which exhibited better compatibility between the organic matrix and inorganic nanofillers. In addition, introduction of MOF particles assisted in significant improvement of hydrophilicity and surface negative charges for the selective layer along with the fouling resistance of the membrane. The MOF-composite membrane exhibited a high pure water permeability ( $6.94 \text{ L m}^{-2} \text{ h}^{-1} \text{ bar}^{-1}$ ) along with a very high rejection of 98.2% and 97.4% at 2 and 4 bars for desalination of NaCl solution. Moreover, the long-term performance of MOF embedded membrane was monitored for 30 days, during which the membrane showed very good durability.

## 7.5. Membrane Distillation

Membrane distillation operates via a thermal desalination method where two adjoined streams of hot saline solution and cold water are separated by a hydrophobic membrane. The temperature difference between the two streams induces a partial pressure gradient and the generated vapor from the saline stream gets transported to the colder side through the membrane in order to balance the partial pressure. In this process, the hydrophobicity of the membrane plays a crucial role as it allows the transportation of only vapor. Hence, the membrane should be maintained as dry.<sup>[188]</sup> The membrane distillation membrane typically prevents the transport of any solid/non-volatile species, which results in the complete accumulation of pure water. To fabricate membrane distillation membranes, the choice of hydrophobic components includes PVDF, polyethylene, polytetrafluoroethylene, and polypropylene, providing several key properties such as high permeability, adequate liquid entry pressure, low membrane fouling, high chemical and thermal stability, and so on.<sup>[100,211]</sup> To this end, the incorporation of hydrophobic MOFs to fabricate the hybrid membrane with enhanced hydrophobicity and porosity has been considered highly promising to achieve efficient desalination performance. In 2017, Chung and co-workers rationalized a strategy to fabricate nature-mimetic hydrophobic membrane via molecular engineering of MIL-53- $\text{NH}_2$ (Al).<sup>[167]</sup> To achieve this, the authors adapted a unique two-step synthetic approach in which the MOF crystals were grown on alumina tube supports and perfluoro molecules were introduced in order to improve hydrophobicity and reduce the surface energy of the MOF surface. Interestingly, the elemental Al from the substrate surface was utilized as active sites for the growth of the MOF which resulted in the formation of nano and hierarchical roughness via surface functionalization of the porous alumina with the MOF. Further, the membrane was found to exhibit very good vacuum distillation flux of  $32.3 \text{ L m}^{-2} \text{ h}^{-1}$  at  $60^\circ\text{C}$  and desalination rejection under optimum conditions. In the next year, Efome

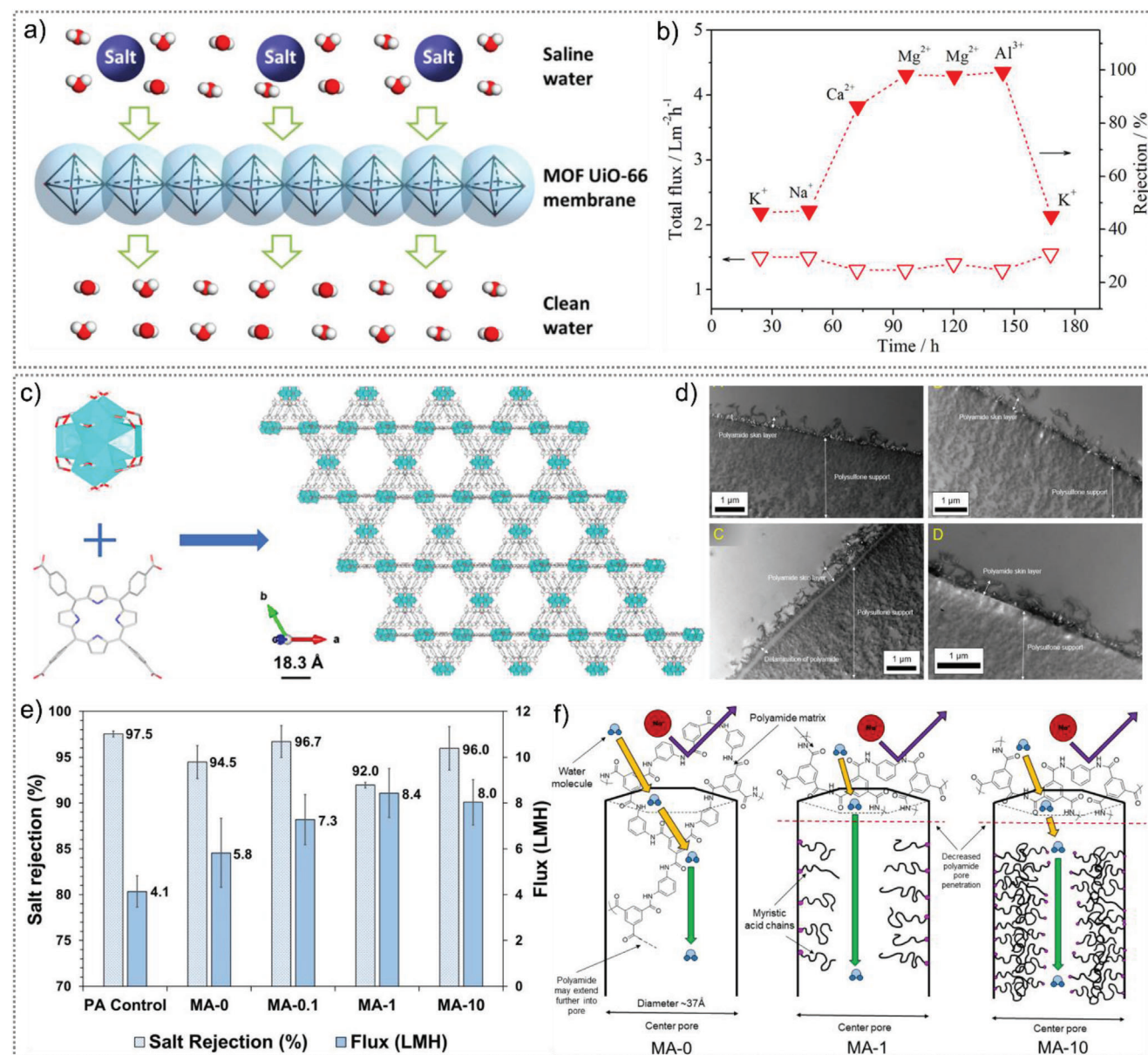


**Figure 11.** a) UiO-66(Zr) Membranes Supported on Alumina Hollow Fibers for Desalination. b) Desalination performance of the UiO-66(Zr) membrane. Five different saline water solutions (containing KCl, NaCl, CaCl<sub>2</sub>, MgCl<sub>2</sub>, or AlCl<sub>3</sub>) with the same concentration (0.20 wt%) were applied as feeds at 20 °C ± 2 °C under a pressure difference of 10.0 bar. Reproduced with permission.<sup>[124]</sup> Copyright 2015, American Chemical Society. c) Metal node of PCN-222 (top left), composed of six Zr<sup>4+</sup> (cyan) links to the TCPP ligand via carboxylate groups in an eight-connected fashion to form a 3D framework with channels aligned along the c-axis. d) TEM images of polyamide membrane, MA-0, MA-0.1, and MA-1 membranes. e) Water flux (LMH) and salt rejection results for (left to right) PA, MA-0, MA-0.1, MA-1, and MA-10 membranes with 2000 ppm NaCl feed and transmembrane pressure of 250 psi. f) Schematic depicting water transport through PCN-222 pores with increasing MA loading. Reproduced with permission.<sup>[208]</sup> Copyright 2020, American Chemical Society.

and co-workers prepared a novel super-hydrophobic nanofiber membrane via electrospinning of Fe-BTC MOF and PVDF on a nonwoven support material for direct contact membrane distillation (Figure 12).<sup>[171]</sup> In addition, a pre-treatment method, namely solvent basing, was applied on the substrate to strengthen the nanofibers. The substrate attachment and loading up to 5 wt% of the MOF were achieved. The as-synthesized membrane exhibited improved hydrophobicity (water contact angle: 138.06° ±

2.18°) along with 99.9% NaCl rejection (35 g.L<sup>-1</sup>) performance in the direct contact membrane distillation process. In 2019, Li, Zie and co-workers came up with a new type of hybrid hollow fiber-enabled hydrophobic MOF/PVDF membrane with Al-Fumarate as MOF.<sup>[212]</sup> The MOF/PVDF exhibited improved water flux along with membrane porosity and thermal efficiency upon addition of the MOF particles. Further, the MOF/PVDF membrane showed excellent desalination durability in high salt

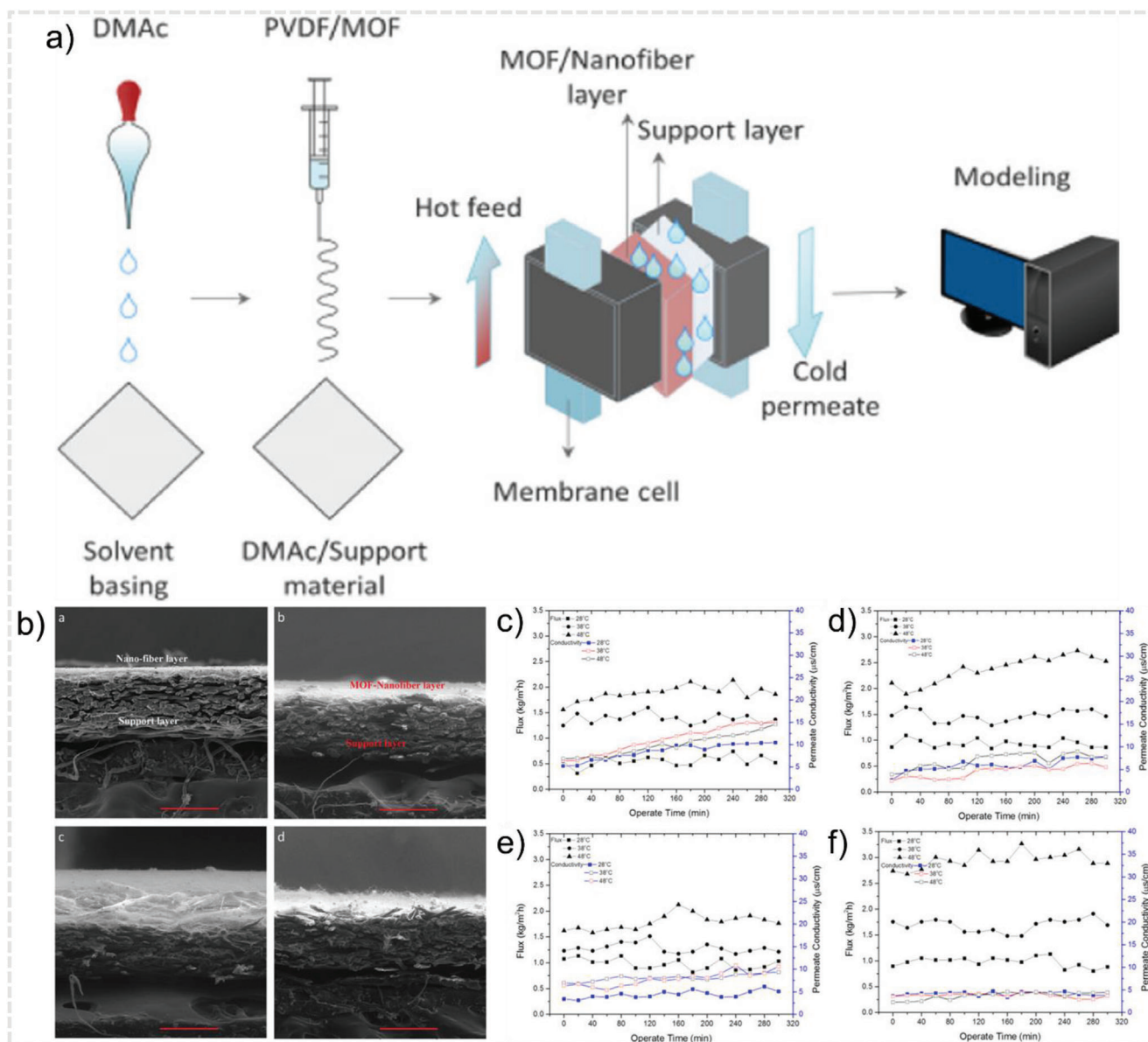


**Figure 12.** a) Schematic illustrations of synthesis for MOF supported on nanofiber for desalination by direct contact membrane distillation. b) SEM images of cross section of PVDF, PV-1, PV-3, and PV-5. Flux and permeate conductivity for c) PVDF, d) PV-1, e) PV-3, and f) PV-5. Reproduced with permission.<sup>[171]</sup> Copyright 2018, American Chemical Society.

rejection (>99.9%) performance for NaCl solution over 50 h. In another report, Rahimpour and co-workers prepared an ultrathin thin film composite membrane with a ZIF-8(Zn)/chitosan layer coated on the PVDF membrane surface for enhanced membrane distillation performance toward water desalination.<sup>[213]</sup> The ZIF-8(Zn)/chitosan layer along with the PVDF membrane was found to contribute to significant enhancement of water entry pressure for the composite membrane. The permeate water flux was found to be increased by 350% upon installation of the ZIF-8/chitosan layer. In addition, the composite membrane showed improved antifouling properties upon treatment with seawater, and very high NaCl rejection (>99.5%) was also achieved. The theoretical calculations revealed good compatibility of the chitosan chain

and ZIF-8(Zn) particles, which resulted in improved membrane distillation performance.

## 7.6. Nanofiltration

Nanofiltration technique is generally employed for removal of larger salts (sized up to 50Å) such as MgCl<sub>2</sub>, Na<sub>2</sub>SO<sub>4</sub>, MgSO<sub>4</sub>, and MgCl<sub>2</sub>. In 2017, Vankelecom and co-workers demonstrated the fabrication of a continuous ZIF-8(Zn) layer via the liquid-liquid interfacial coordination method on a porous polyether-sulfone surface.<sup>[214]</sup> During the fabrication process, the authors investigated the role of different parameters including



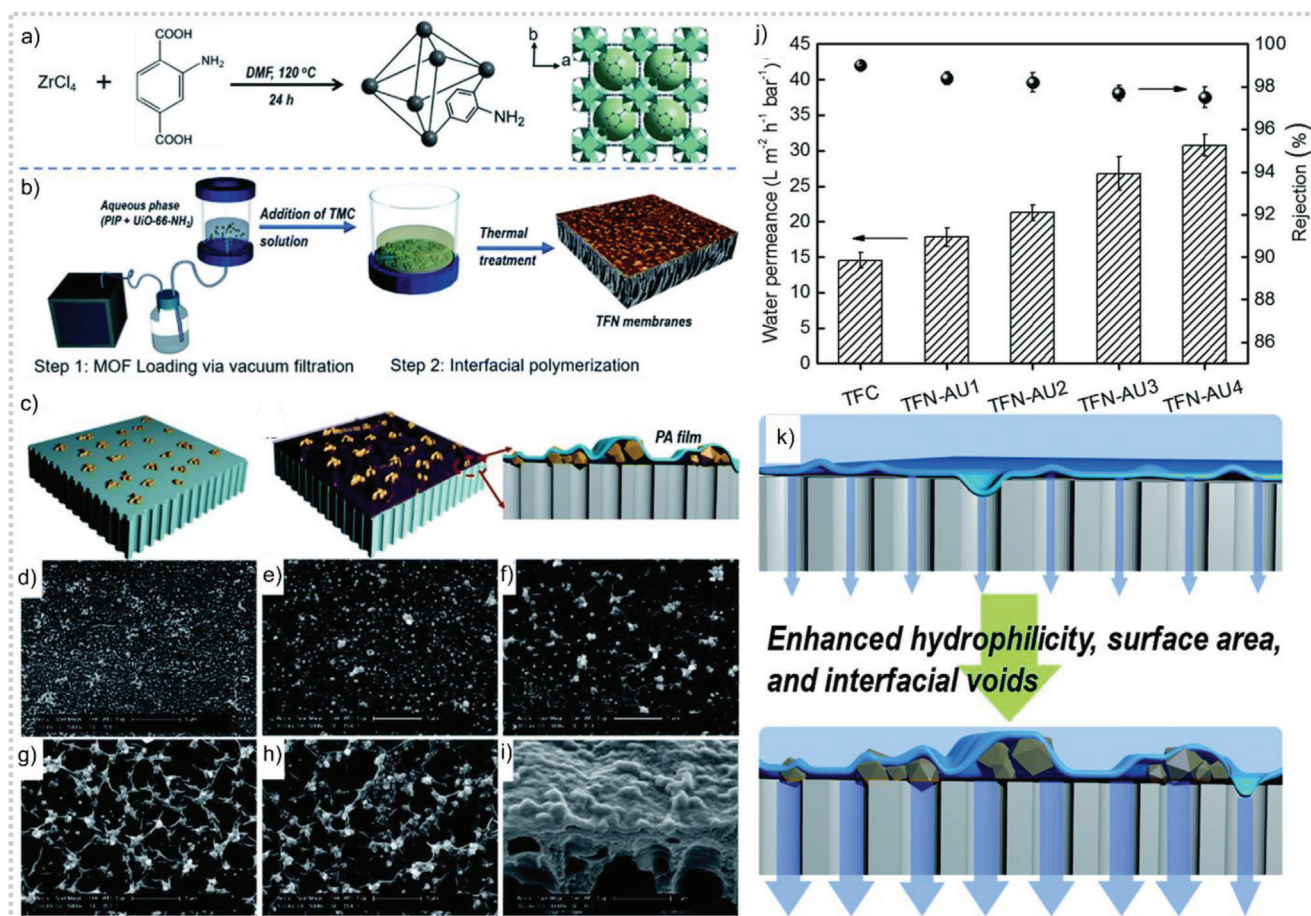


**Figure 13.** a) Synthesis of UiO-66-NH<sub>2</sub>(Zr) nanocrystals and b) preparation process of thin film nanocomposite membranes assisted by filtration of the aqueous phase prior to interfacial polymerization. c) Evolution procedure of UiO-66-NH<sub>2</sub>(Zr) functionalized TFN membranes: MOF loading onto membrane substrates via vacuum assisted filtration and schematic illustration of forming a crumpled polyamide surface and cross-section after the interfacial polymerization reaction with trimesoylchloride. SEM images of the as-prepared polyamide membranes with different ZrMOF loading mass: d) 0 mg cm<sup>-2</sup>, e) 6.8 mg cm<sup>-2</sup>, f) 10.3 mg cm<sup>-2</sup>, g) 13.7 mg cm<sup>-2</sup>, and h) 20.5 mg cm<sup>-2</sup>. Scale bar is 5 μm. i) Cross-sectional images of the TFN-AU4 membrane. Scale bar is 1 μm. j) Pure water permeance and salt rejection of thin film composites and TFN membranes prepared with different UiO-66-NH<sub>2</sub>(Zr) loading mass (Na<sub>2</sub>SO<sub>4</sub> concentration: 1.5 g L<sup>-1</sup>; applied pressure: 4 bar). k) The proposed mechanism of enhanced water transport through the crumpled MOF/PA membranes. Reproduced with permission.<sup>[217]</sup> Copyright 2019, The Royal Society of Chemistry.

precursor concentrations, reaction time, and support in the formation of the ZIF-8(Zn) membrane which revealed that utilization of higher concentration of MOF precursors can result in denser ZIF-8(Zn) membranes with less defects. Moreover, it was observed that by varying the precursors' concentration, the overall nanofiltration performance of the membrane could be tuned. In another work, Liu, Gao and co-workers reported post-synthetic modification of UiO-66-NH<sub>2</sub>(Zr) nanoparticles with palmitoyl chloride to improve the dispersy of the MOF particles within the polyamide layer to prepare thin film nanocomposite nanofiltration membranes.<sup>[215]</sup> The MOF-embedded membranes exhibited "ridge-valley" morphology along with higher water permeability and lower rejection. Moreover, it showed improved pure water flux from 8.1 to 12.4 L m<sup>-2</sup> h<sup>-1</sup> bar<sup>-1</sup> with Na<sub>2</sub>SO<sub>4</sub> rejection of 95%. In an interesting work, Navarro and co-workers came up with an innovative technique to install MIL-101(Cr) nanoparticles in thin film nanocomposite membranes via transferring a Langmuir-Schaefer film of the MOF in between the asym-

metric polyimide support at the bottom and the top polyamide thin layer.<sup>[216]</sup> In comparison with the conventional synthetic methods, this methodology involves a very little amount of MOF (3.8 μg cm<sup>-2</sup>), along with results in fabrication of a homogeneously coated, defect-free ultrathin MOF membrane. Further, the fabricated membrane exhibited very good nanofiltration performance toward methanol/dye solutions which was correlated with the large pore system and hydrophilic nature of MIL101(Cr), which eventually resulted in higher methanol transport and excellent dye rejection performance. In 2019, Zhang and co-workers used UiO-66-NH<sub>2</sub>(Zr) nanoparticles as functional fillers to fabricate polyamide composite membranes (Figure 13).<sup>[217]</sup> To achieve this, an aqueous solution of evenly dispersed UiO-66-NH<sub>2</sub>(Zr) and piperazine was positioned on a membrane through vacuum filtration, which was further employed for subsequent interfacial polymerization with trimesoyl chloride. A stable dispersion of MOF particles in the layer was observed owing to the covalent linking between the trimesoylchloride moieties and

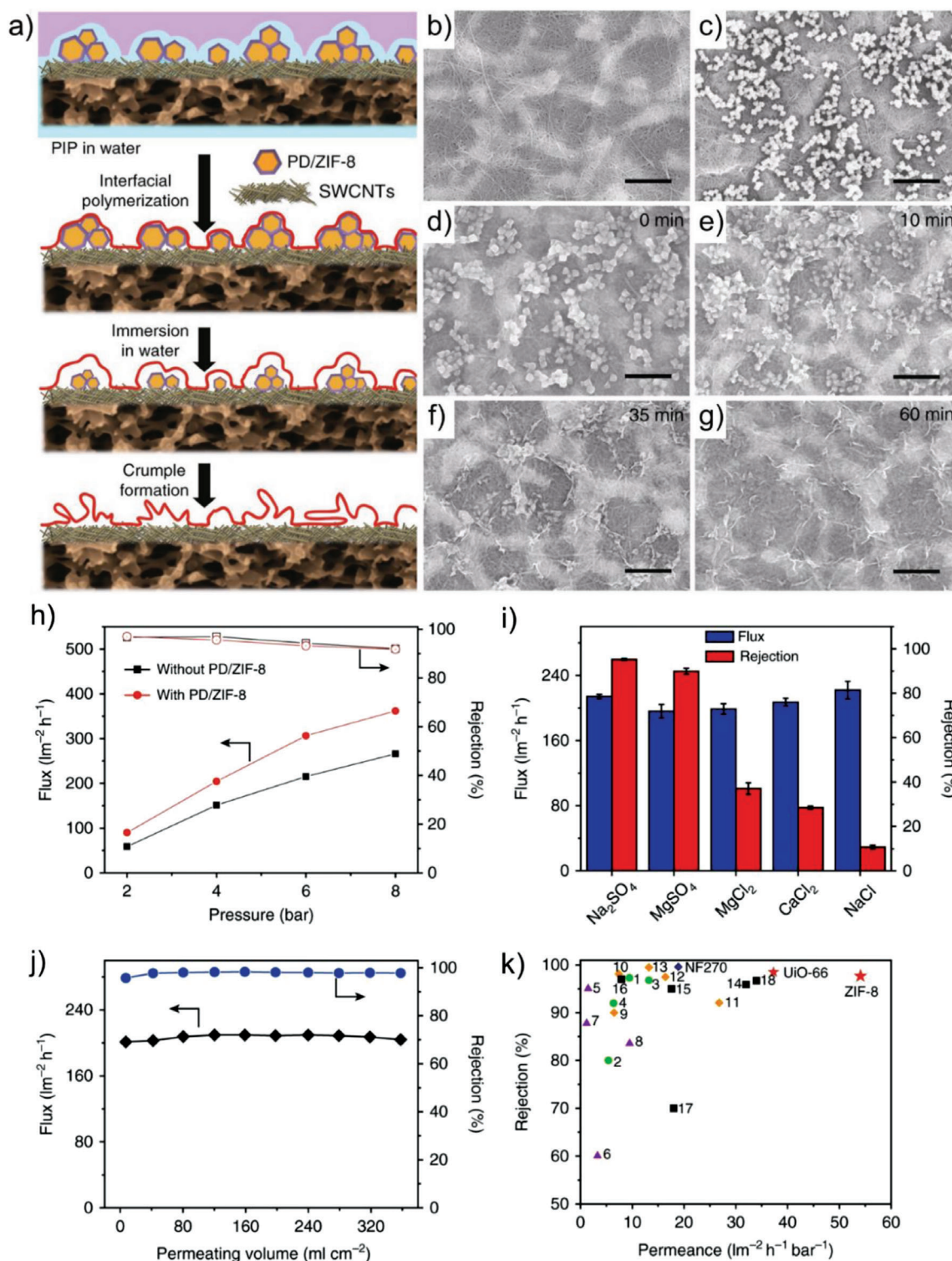


**Figure 14.** a) A schematic illustration showing the preparation process of nanoparticles induced crumpled PA NF membrane. Top-view SEM images of different composite membranes: b) pristine SWCNTs/PES composite membrane. c) PD/ZIF-8 nanoparticles loaded SWCNTs/PES composite membrane. d–g) Morphology change of the membrane immersed into water in different time after interfacial polymerization reaction on PD/ZIF-8 nanoparticles loaded SWCNTs/PES composite membrane. h) Flux and rejection of the PA NF membranes prepared from the SWCNTs/PES composite membrane with and without PD/ZIF-8 nanoparticles loading with respect to applied pressure. i) Variation of flux and rejection of PA NF membranes prepared from PD/ZIF-8 nanoparticles loaded SWCNTs/PES composite membrane with respect to different salt solutions. j) Variation of flux and rejection of PA NF membrane prepared from PD/ZIF-8 nanoparticles loaded SWCNTs/PES composite membrane as a function of permeating volume. k) Summary of the filtration performance of the state-of-the-art NF membranes reported in literature in consideration of permeance and rejection for  $\text{Na}_2\text{SO}_4$ . Reproduced with permission.<sup>[218]</sup> Copyright 2018, Nature Publishing Group.

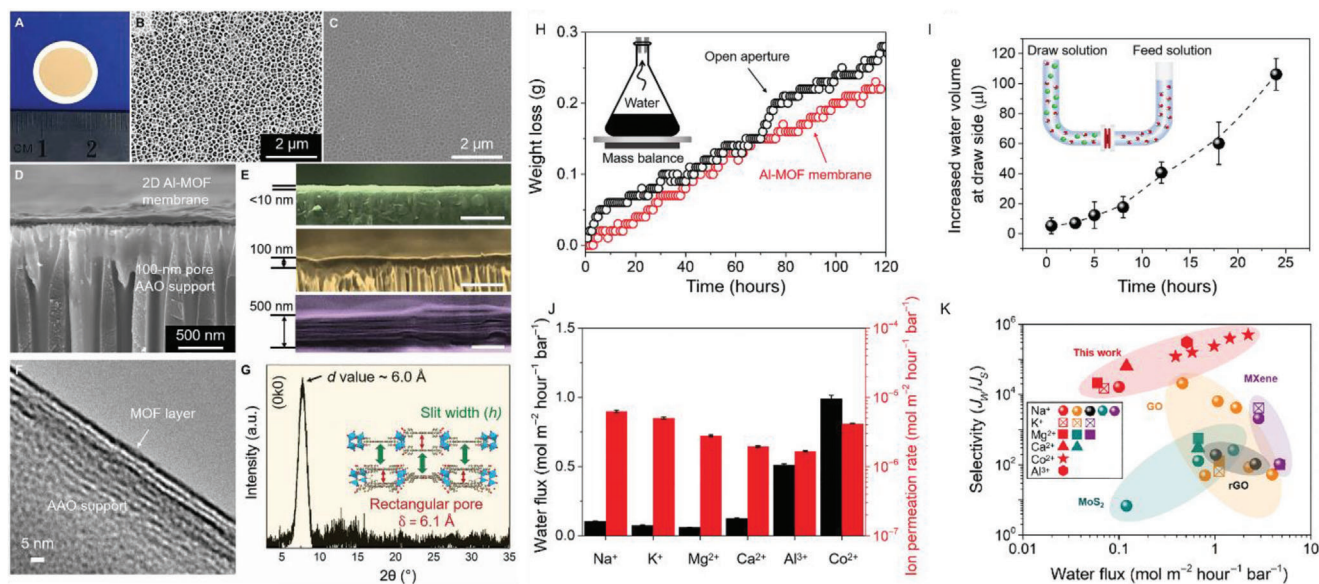


**Figure 15.** A) Digital photo of an as-prepared 100-nm-thick Al-MOF laminar membrane on AAO substrate. B) SEM image of a bare AAO substrate. C) SEM image of a sub-10-nm-thick Al-MOF laminar membrane on AAO substrate. The visibility of the substrate background elucidates the ultrathin coverage. D) Cross-sectional overview of a 100-nm-thick Al-MOF laminar membrane on AAO substrate. E) Magnified cross-sectional views of 2D Al-MOF membranes with different thicknesses. Membranes less than 100 nm (green and gold) present a compact stacking, whereas the membrane at a thickness of 500 nm (purple) apparently shows a typical laminar structure. Scale bars, 500 nm. F) Cross-sectional TEM image of the 2D Al-MOF laminar membrane. G) GIXRD pattern of the Al-MOF laminar membrane. Reproduced with permission.<sup>[219]</sup> Copyright 2020, American Association for the Advancement of Science.

the terminal  $\text{NH}_2$  groups of  $\text{UiO-66-NH}_2(\text{Zr})$ . In addition, the positioned  $\text{UiO-66-NH}_2(\text{Zr})$  particles were found to generate a fishnet-like polyamide surface and a looser layer. Such a unique composite structure of the membrane was found to result in enhanced water transport properties, while maintaining the salt rejection performance. In addition, the best performing thin film nanocomposite membrane (with  $20.5 \text{ mg cm}^{-2}$  as mass loading) showed excellent water permeability and  $\text{Na}_2\text{SO}_4$  rejection of 97.5%. In another interesting work, Zhu, Jin and co-workers demonstrated the utilization of ZIF-8(Zn) nanoparticles as sacrificial template to synthesize a thin film composite nanofiltration membrane with a crumpled polyamide layer via interfacial polymerization on a single wall carbon nanotubes composite support (Figure 14a–g).<sup>[218]</sup> The incorporation of the ZIF-8(Zn) nanoparticles resulted in the formation of a crumpled nanostructure with a rough polyamide active layer. In addition, the composite membrane having PD/ZIF-8(Zn) exhibited excellent permeance of  $53.5 \text{ L m}^{-2} \text{ h}^{-1} \text{ bar}^{-1}$  along with a high  $\text{Na}_2\text{SO}_4$  rejection of 95.3%; the ZIF-67(Zn) counterpart was found to show higher water flux ( $1831 \text{ L m}^{-2} \text{ h}^{-1}$ ) with excellent  $\text{Na}_2\text{SO}_4$  rejection of 97.2% (Figure 14h–k). In 2019, Huang and co-workers carried out a comprehensive evaluation of the role of MOFs toward structure–properties correlation of polyamide thin film nanocomposite membranes.<sup>[160]</sup> Three water-stable MOFs, namely ZIF-8(Zn), MIL-53(Al), and  $\text{UiO-66-NH}_2(\text{Zr})$  were utilized to fabricate the thin film nanocomposite membrane via preloading interfacial polymerization and blending interfacial polymerization methods. The MOF incorporated membranes were found to possess higher surface negativity along with a thicker polyamide layer and rougher surface. The introduction of MOF particles significantly improved the water permeability of thin film nanocompos-

ite membranes in comparison with the corresponding thin film composite membranes and enabled to maintain their selectivity in rejection of xylose (>65%) and NaCl (>40%).

## 7.7. Other Methods

Apart from the above-mentioned well-known desalination methods, recent years have witnessed the development of various novel and innovative approaches for the utilization of MOFs in desalination. In this regard, physical properties of the sorbate molecules such as electrostatic-repulsion or size-selective sieving have been employed. In an exemplary work, Wang and co-workers demonstrated the utilization of a sunlight-responsive MOF for sustainable water desalination.<sup>[137]</sup> The sunlight-responsive MOF material was synthesized by incorporating poly(spiropyran acrylate) (PSP) molecules inside the pores of MIL-53(Al) followed by in situ polymerization. MIL-53(Al) was selected as the host matrix because of its well-known breathing effect along with high hydrolytic stability. In addition, the authors strategically utilized spiropyran (SP) as the photo-responsive guest molecule which could be converted to its zwitterionic state, namely merocyanine (MC) under UV light irradiation or dark conditions. As expected, the introduction of SP inside MIL-53 was found to result in an expansion of the pores of the MIL-53(Al) up to  $\approx 8.5 \text{ \AA}$ . Further, the PSP-MIL-53(Al) exhibited reversible capture and release of salts in water under UV light irradiation and dark conditions as the poly(spiropyran acrylate) unit transformed into its' zwitterionic PMC form. This subsequently resulted in anion adsorption by the cationic indolium groups and cation adsorption by the anionic phenolate groups in 30 min

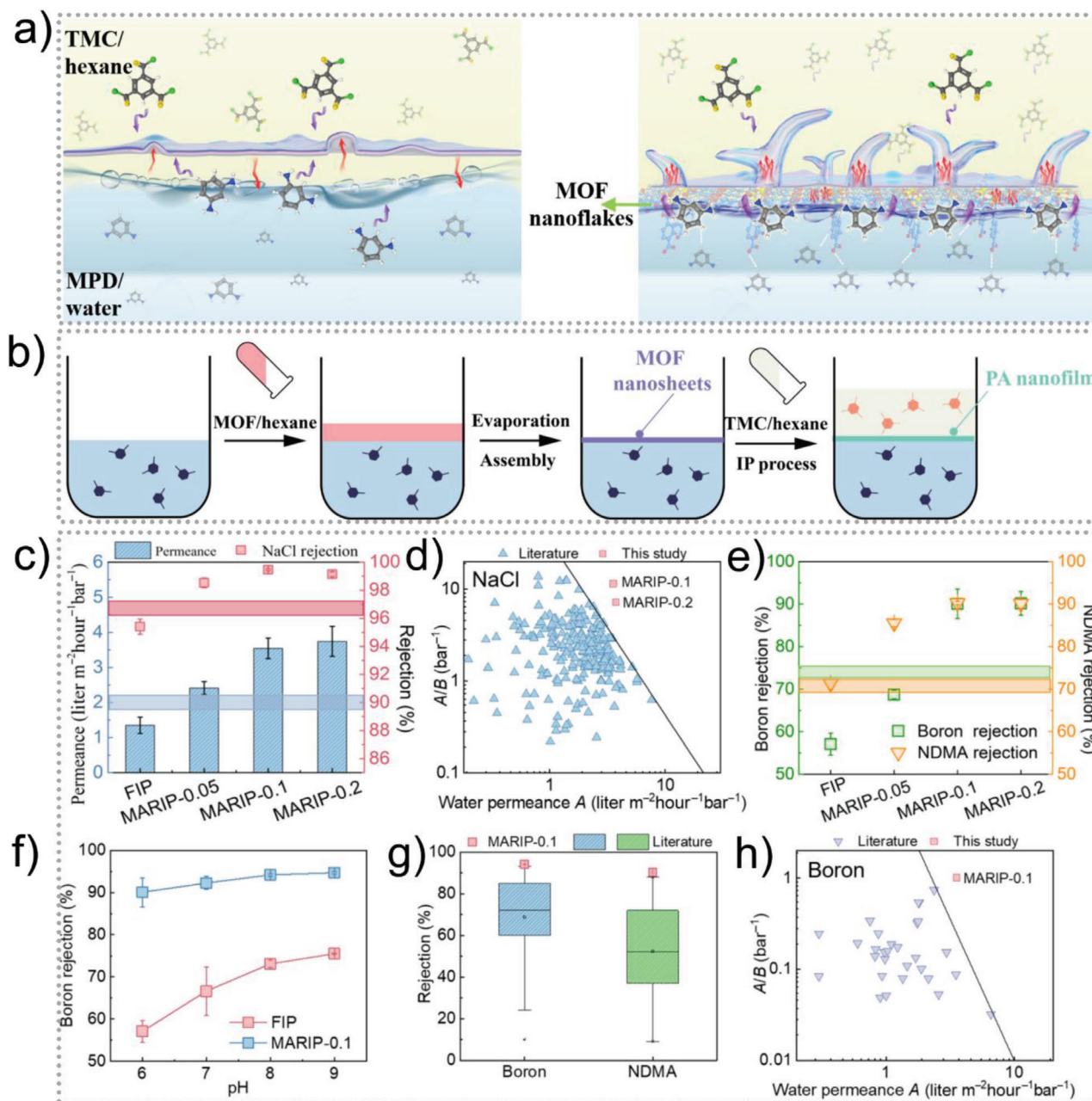


**Figure 16.** a) Graphical illustration of the interfacial polymerization process at a free interface (free interface polymerization [FIP]). b) Experimental procedure for MARIP: an MOF/hexane solution was spread onto the surface of an aqueous m-phenylenediamine solution; self-assembly of MOF formed at the water surface after hexane evaporation; a hexane solution of trimesoylchloride was then added to the self-assembled MOF film to initiate interfacial polymerization, and the obtained polyamide nanofilm was transferred to the support membrane for further analysis and testing. c) Pure water permeance and NaCl rejection. d) Separation performance in terms of water permeance and water/NaCl selectivity of MARIP-0.1 and MARIP-0.2 membranes (red) as compared with literature data (blue). e) Rejection of boron, f) rejection of boron ( $5 \text{ mg liter}^{-1}$ , 16 bar,  $24^\circ\text{C}$ ) by FIP and MARIP-0.1 membranes at different pH. g) Comparison of the boron (pH 8) and NDMA rejection performance of MARIP-0.1 with data reported in literature. h) Separation performance in terms of water permeance and water/boron selectivity of MARIP-0.1 membrane (red) as compared with literature data (purple). Reproduced with permission.<sup>[220]</sup> Copyright 2022, American Association for the Advancement of Science.

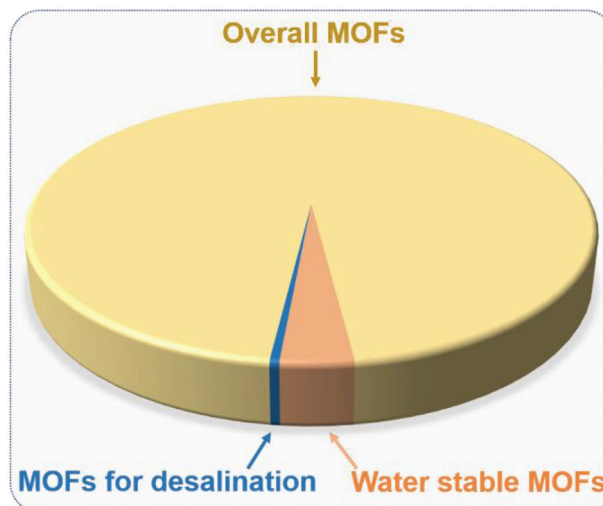
from water. In turn, upon sunlight illumination, the MC isomers were established to reverse back to the SP configuration, resulting in rapid release of the adsorbed salts within just 4 min. The removal ability of the MOF system was tested via a single-column setup in dark conditions. PSP-MIL-53 showed excellent

ion removal performance in the single-column setup, which was found to be more efficient than the batch sorption experiments. The single-column setup allowed very good flowability of the suspension and also showed very good recyclability under dark conditions and room lighting stimulation. Further, PSP-MIL-53(Al)

also performed significantly to remove the ions from the synthetic sea waters and it registered a very low energy consumption ( $0.11 \text{ Wh L}^{-1}$  for 2,233 ppm synthetic brackish water, with a  $139.5 \text{ l kg}^{-1} \text{ d}^{-1}$  freshwater production). Such energy economic strategies can propel the development of more such functional materials responsive toward renewable solar energy and improve the sustainability of water desalination. In 2020, Zhang and co-workers presented the first example of the successful exfoliation of 2D monolayer aluminum tetra-(4-carboxyphenyl) porphyrin framework, namely Al-MOF nanosheets (Figure 15).<sup>[219]</sup> The exfoliated nanosheets were employed as the building blocks to fabricate the ultrathin Al-MOF membranes. Al-MOF nanosheets showed very good structural robustness toward the water and were found to form a laminar membrane through facile vacuum filtration process. Further, the 2D Al-MOF displayed water fluxes up to  $2.2 \text{ mol m}^{-2} \text{ h}^{-1} \text{ bar}^{-1}$  with an extremely low permeability of  $\approx 3.3 \times 10^{-6} \text{ mol m}^{-2} \text{ h}^{-1} \text{ bar}^{-1}$ ) and 100% rejection rates toward inorganic ions. The density functional theory calculations confirmed the dictating contribution of the intrinsic nanopores of the Al-MOF nanosheets and the vertical alignments of the channels toward the transportation of water molecules. In 2021, Lui and co-workers prepared continuous Al-based MOF-membranes upon  $\alpha\text{-Al}_2\text{O}_3$  substrates via in situ hydrothermal synthesis.<sup>[135]</sup> The continuous polycrystalline MOF-303(Al) membranes showed very good rejection toward divalent ions, for example, it registered a rejection performance of 93.5% and 96.0% for  $\text{MgCl}_2$  and  $\text{Na}_2\text{SO}_4$ , respectively. The ion rejection was attributed to the size-selective sieving and electrostatic-repulsion ability of MOF-303(Al) membranes. It showed excellent water permeability of  $3.0 \text{ L.m}^{-2} \text{ h}^{-1} \text{ bar}^{-1} \cdot \mu\text{m}$ . In addition, the MOF-303(Al) membranes exhibited good stability and less costs of production in comparison to other standard membranes. In recent efforts by Lin, Tang, Wang, and co-workers have demonstrated the fabrication of MOF nanoflakes-based ultraselective polyamide membrane (Figure 16a,b).<sup>[220]</sup> Cu-BDC (copper-1,4-benzene dicarboxylate) MOF nanoflakes having amphiphilic nature were used owing to their merits such as high aspect ratio, nanosize, large porosity, and asymmetric wettability. Further, a unique technique, namely MOF Assembly Regulated Interfacial Polymerization was employed to fabricate highly cross-linked polyamide membranes. The membranes showed significantly improved water permeance ( $\approx 125\%$  enhancement) in comparison with the commercial thin film composite-polyamide membranes. The membranes also exhibited very high rejection performance of  $94.2\% \pm 0.2\%$  toward boron at pH 8 and  $90.3\% \pm 0.4\%$  toward N-nitrosodimethylamine (Figure 16c–h).

## 8. Conclusion and Future Outlook

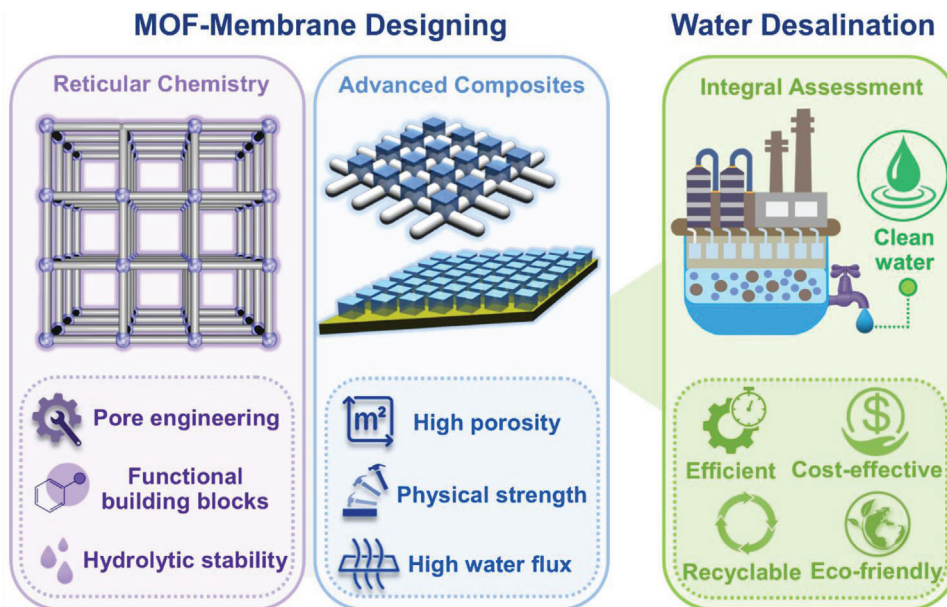
Fresh water scarcity is one of the most critical environmental issues of the 21st century globally. Extensive research activities are going on to obtain green, sustainable, and energy-economic solutions to address this challenge. To this end, different water desalination techniques have already shown tremendous promise as the potential alternative of the ground water resources. Hence, the development of efficient materials and methods to enhance the desalination efficiency in terms of lower energy consumption, lower cost, and environmentally friendliness is currently a research hotspot. MOFs are very promising candidates to im-



**Scheme 4.** Comparison of number of articles with the keywords “Metal–organic Frameworks,” “Water stable Metal–organic Frameworks,” and “Metal–organic Frameworks desalination” (source: Scopus), highlighting the untouched opportunity in MOFs for desalination.

prove the efficiency of different desalination processes including forward osmosis, reverse osmosis, membrane distillation, and capacitive deionization, when they are included as a functional components into polymeric or ceramic membranes. In this review, we have provided an overview of current developments in MOFs and MOF-based membranes from the perspective of material design and chemical encoding approach, synthetic methods, mechanistic insights, and their applicability toward different desalination processes. Owing to their ordered and tunable porous structures, controlled surface, and morphological properties, MOFs have been an appealing choice to be integrated into composite membranes for desalination. The channeled porous structure of MOFs aids to improve the permeability of classic polymeric and ceramics membranes whilst enabling controlling of the ion-migration selectivity and capacity of the membrane. This counterintuitive combination is possible because the pore-space of the MOF materials can be finally controlled to achieve ion-size exclusion or ion-specific chemical interactions. The combination of MOFs with various desalination membranes promises to be one of the future solutions to palliate the clean water scarcity.

Despite the exceptional accomplishments of MOFs as functional materials in diverse applications, their performance for desalination treatment is still understudied and their true potential is yet to be exploited. As evident in Scheme 4, very few MOFs have been utilized for desalination which renders in immense window of opportunity to exploit other water stable MOFs with different functionalities for desalination. There are still a few key issues that need to be addressed in order to develop large-scale MOF-based systems for desalination treatments. Among these bottlenecks are the stability and durability of the MOFs themselves in extreme realistic conditions, which makes it challenging to translate the existing accomplishments to the practical implementation level. Moreover, the processing of MOF-based membrane materials and their applicability in real-world water treatment plants is still in early stages, and significantly more



**Scheme 5.** Perspectives to improve the performance of MOF-based materials toward water desalination considering the possible advances from the material design and application demand.

scientific and engineering knowledge has to be acquired. In order to make future large-scale processes affordable and viable, it is also necessary to devote more efforts need toward bulk-scale, cost-efficient production of MOFs (Scheme 5).

As MOFs are usually integrated as nanoparticles in membrane devices, research on size and shape control of the nanoparticles along with their mechanical binding stability to the polymeric/ceramic membranes are of paramount importance. In addition, the ecotoxicity aspects of both the MOF and polymeric components need to be considered. It should be assured that in case of lesser long-term physiochemical stability of the MOFs, the impact of the individual components on the environment should be minimal. In this regard, fabrication of MOFs with green and abundant components, specially the organic linker constituents (e.g., isophthalic acid, furanic acid, fumaric acid, aspartic or gluconic acids) and their synthesis via low temperature water-based protocols is highly recommended and gaining attention in the research community. Particularly, utilization of organic solvents hinders sustainability toward green synthesis of industrial-scale production and they also need to be handled with caution and controlled manner (e.g., non-flammable areas). In addition, utilization of organic solvents during the synthesis of polycrystalline MOF membranes not only contributes to high capital footprint but also generates a huge amount of toxic wastes which can have adverse effects to the environment. In contrast, MOF synthesis with water as solvent is considered as the safest, cost-effective, and simplest post-treatment method. Apart from that, synthesis of MOFs and MOF-based membranes via solvent-free methods has been attracting scientific attention for the large-scale production of MOF-based compounds in a green pathway.

The potentials of reticular chemistry for desalination purposes are yet to be definitely applied for water desalination (Scheme 5). Up to date, several MOFs have been integrated within desalination membranes, but the chemical encoding of their pore space

has been quite limited, even though it can play an important role to boost the water migration and engineer ion-selective gates within their pore space. Delamination of MOFs as graphene like Metal–Organic Layers or the processing of MOFs as printable gel materials is quite an interesting processing protocol to transfer to the integration and production of MOF-based desalination membranes. In addition, reticular materials hold the possibility to integrate additional functions that could boost the desalination process, as are the ones of photo, chemo, or enzymatic like catalytic degradation of organic persistent pollutants.

From the desalination point of view, several challenges such as high energy, environmental damage while disposing the concentrated salt water, and so on still need to be addressed. It is important to have in mind that desalination is quite expensive; so, any coupling of desalination to water remediation or critical raw elements recovery would add a parallel value to the process to lower its overall costs. Today, critical raw elements mining from brines, seawater, acid drainages, or industrial waste water sources is gaining more and more attention, and an ion-selective desalination could give the answer to clean water and critical raw elements production. Here, MOFs could bring the ion-selectivity needed to achieve the goal. Only through the joint efforts of researchers from different expertise, including chemistry, materials science, engineering, physics, and environmental science, rapid progress can be made in the field of MOF-based materials for desalination applications, enabling a viable future for the next generations on Earth.

## Acknowledgements

This work was supported by the Spanish State Research Agency (MCIN/AEI/10.13039/501100011033) and the European Regional Development Fund (ERFD) through the projects PID2019-108028GB-C21, TED2021-129810B-C22, and PID2020-15935RB-C42. The European

Union's Horizon 2020 research and Innovation programme is also acknowledged for the funding of the LC-SC3-RES-25-2020 4AirCRAFT (Ref.: 101022633) project. In addition, 4AirCRAFT project was also supported by the Japan Science and Technology Agency (JST) and the Mission Innovation Challenge was supported by the Sao Paulo Research Foundation (FAPESP).

## Conflict of Interest

The authors declare no conflict of interest.

## Keywords

desalination, drinking water, environment, membranes, MOFs, pollutants removal, water purification

Received: April 30, 2023

Revised: July 6, 2023

Published online:

- [1] M. A. Shannon, P. W. Bohn, M. Elimelech, J. G. Georgiadis, B. J. Mariñas, A. M. Mayes, *Nature* **2008**, 452, 301.
- [2] C. J. Vörösmarty, P. Green, J. Salisburry, R. B. Lammers, *Science* **2000**, 289, 284.
- [3] P. C. D. Milly, J. Betancourt, M. Falkenmark, R. M. Hirsch, Z. W. Kundzewicz, D. P. Lettenmaier, R. J. Stouffer, *Science* **2008**, 319, 573.
- [4] S. Rojas, P. Horcajada, *Chem. Rev.* **2020**, 120, 8378.
- [5] *Resolution A/RES/64/292*, United Nations General Assembly, **2010**.
- [6] P. A. Kobielska, A. J. Howarth, O. K. Farha, S. Nayak, *Coord. Chem. Rev.* **2018**, 358, 92.
- [7] S. Dutta, S. Let, S. Sharma, D. Mahato, S. K. Ghosh, *Chem. Rec.* **2021**, 21, 1666.
- [8] I. Ali, *Chem. Rev.* **2012**, 112, 5073.
- [9] S. B. Grant, J.-D. Saphores, D. L. Feldman, A. J. Hamilton, T. D. Fletcher, P. L. M. Cook, M. Stewardson, B. F. Sanders, L. A. Levin, R. F. Ambrose, A. Deletic, R. Brown, S. C. Jiang, D. Rosso, W. J. Cooper, I. Marusic, *Science* **2012**, 337, 681.
- [10] M. Patel, R. Kumar, K. Kishor, T. Mlsna, C. U. Pittman, Jr., D. Mohan, *Chem. Rev.* **2019**, 119, 3510.
- [11] Population Division, United Nations **2015**.
- [12] M. Mon, R. Bruno, J. Ferrando-Soria, D. Armentano, E. Pardo, *J. Mater. Chem. A* **2018**, 6, 4912.
- [13] J. Canivet, A. Fateeva, Y. Guo, B. Coasne, D. Farrusseng, *Chem. Soc. Rev.* **2014**, 43, 5594.
- [14] P. S. Goh, A. F. Ismail, *Desalination* **2018**, 434, 60.
- [15] A. F. Ismail, M. Padaki, N. Hilal, T. Matsuura, W. J. Lau, *Desalination* **2015**, 356, 140.
- [16] N. Abdullah, N. Yusof, A. F. Ismail, W. J. Lau, *Desalination* **2021**, 500, 114867.
- [17] J. Eke, A. Yusuf, A. Giwa, A. Sodiq, *Desalination* **2020**, 495, 114633.
- [18] *Global Water Intelligence, Desalination plants, Desaldata, 2020*, <https://www.desaldata.com/>.
- [19] E. Jones, M. Qadir, M. T. H. van Vliet, V. Smakhtin, S. Kang, *Sci. Total Environ.* **2019**, 657, 1343.
- [20] D. Zarzo, D. Prats, *Desalination* **2018**, 427, 1.
- [21] C. Fritzmam, J. Löwenberg, T. Wintgens, T. Melin, *Desalination* **2007**, 216, 1.
- [22] M. Al-Shammiri, M. Safar, *Desalination* **1999**, 126, 45.
- [23] M. A. Darwish, N. M. Al-Najem, *Appl. Therm. Eng.* **2000**, 20, 399.
- [24] E. K. Summers, H. A. Arafat, J. H. Lienhard V, *Desalination* **2012**, 290, 54.
- [25] *National Research Council (US) Committee on Advancing Desalination Technology and National Academies Press (US) 2008 Desalination: A National Perspective*, vol. xiv, National Academies Press, Washington, DC, p. 298.
- [26] T. Humplik, J. Lee, S. C. O'Hern, B. A. Fellman, M. A. Baig, S. F. Hassan, M. A. Atieh, F. Rahman, T. Laoui, R. Karnik, *Nanotechnology* **2011**, 22, 292001.
- [27] J. Cadotte, *U. S. Patent 4, 277, 344*, **1981**.
- [28] M. Kadhom, B. Deng, *Appl. Mater. Today* **2018**, 11, 219.
- [29] H. Dong, L. Zhao, L. Zhang, H. Chen, C. Gao, W. S. Winston Ho, *J. Membr. Sci.* **2015**, 476, 373.
- [30] M. L. Lind, A. K. Ghosh, A. Jawor, X. Huang, W. Hou, Y. Yang, E. Hoek, *Langmuir* **2009**, 25, 10139.
- [31] C. L. Kong, T. Shintani, T. Tsuru, *New J. Chem.* **2010**, 34, 2101.
- [32] H. Huang, X. Qu, H. Dong, L. Zhang, H. Chen, *RSC Adv.* **2013**, 3, 8203.
- [33] H. Huang, X. Qu, X. Ji, X. Gao, L. Zhang, H. Chen, L. Hou, *J. Mater. Chem. A* **2013**, 1, 11343.
- [34] H. Dong, X. Y. Qu, L. Zhang, L. H. Cheng, H. L. Chen, C. J. Gao, *Desalin. Water Treat.* **2011**, 34, 6.
- [35] L. Li, J. Dong, T. M. Nenoff, R. Lee, *J. Membr. Sci.* **2004**, 243, 401.
- [36] M. Kadhom, J. Yin, B. Deng, *Membranes* **2016**, 6, 50.
- [37] J. Yin, E. Kim, J. Yang, B. Deng, *J. Membr. Sci.* **2012**, 423–424, 238.
- [38] H. Wu, B. Tang, P. Wu, *J. Membr. Sci.* **2013**, 428, 341.
- [39] X. Ma, N. Lee, H. Oh, J. Hwang, S. Kim, *Nanoscale Res. Lett.* **2010**, 5, 1846.
- [40] A. Tiraferri, Y. Kang, E. P. Giannelis, M. Elimelech, *Appl. Mater. Interfaces* **2012**, 4, 5044.
- [41] G. L. Jadav, P. S. Singh, *J. Membr. Sci.* **2009**, 328, 257.
- [42] D. Emadzadeh, W. J. Lau, T. Matsuura, A. F. Ismail, M. Rahbari-Sisakht, *J. Membr. Sci.* **2014**, 449, 74.
- [43] M. Yadaa, Y. Inouea, G. Akihitoa, I. Nodab, T. Torikaia, T. Wataria, T. Hotokebuchi, *Colloids Surf., B* **2010**, 80, 116.
- [44] D. Emadzadeha, W. J. Laua, T. Matsuura, N. Hilal, A. F. Ismail, *Desalination* **2014**, 348, 82.
- [45] K. E. Tettey, M. Q. Yee, D. Lee, *Appl. Mater. Interfaces* **2010**, 2, 2646.
- [46] H. Dou, M. Xu, B. Wang, Z. Zhang, G. Wen, Y. Zheng, D. Luo, L. Zhao, A. Yu, L. Zhang, Z. Jiang, Z. Chen, *Chem. Soc. Rev.* **2021**, 50, 986.
- [47] Q. Qian, P. A. Asinger, M. J. Lee, G. Han, K. M. Rodriguez, S. Lin, F. M. Benedetti, A. X. Wu, W. S. Chi, Z. P. Smith, *Chem. Rev.* **2020**, 120, 8161.
- [48] L. Yang, S. Qian, X. Wang, X. Cui, B. Chen, H. Xing, *Chem. Soc. Rev.* **2020**, 49, 5359.
- [49] J. Li, H. Wang, X. Yuan, J. Zhang, J. W. Chew, *Coord. Chem. Rev.* **2020**, 404, 213116.
- [50] O. Shekhhah, J. Liu, R. A. Fischer, C. Wöll, *Chem. Soc. Rev.* **2011**, 40, 1081.
- [51] S. R. Batten, N. R. Champness, X.-M. Chen, J. Garcia-Martinez, S. Kitagawa, L. Ohrstrom, M. O'Keeffe, M. P. Suh, J. Reedijk, *Pure Appl. Chem.* **2013**, 85, 1715.
- [52] H. Furukawa, K. E. Cordova, M. O'keeffe, O. M. Yaghi, *Science* **2013**, 341, 6149.
- [53] R. Ettliger, U. Lächelt, R. Gref, P. Horcajada, T. Lammers, C. Serre, P. Couvreur, R. E. Morris, S. Wuttke, *Chem. Soc. Rev.* **2022**, 51, 464.
- [54] F. Ahmadijokani, H. Molavi, A. Bahi, R. Fernández, P. Alae, S. Wu, S. Wuttke, F. Ko, M. Arjmand, *Adv. Funct. Mater.* **2022**, 32, 2207723.
- [55] M. Lismont, L. Dreesen, S. Wuttke, *Adv. Funct. Mater.* **2017**, 27, 1606314.
- [56] S. Zhou, O. Shekhhah, A. Ramírez, P. Lyu, E. Abou-Hamad, J. Jia, J. Li, P. M. Bhatt, Z. Huang, H. Jiang, T. Jin, G. Maurin, J. Gascon, M. Eddaoudi, *Nature* **2022**, 606, 706.
- [57] R. Freund, O. Zaremba, G. Arnauts, R. Ameloot, G. Skorupskii, M. Dincă, A. Bavykina, J. Gascon, A. Ejsmont, J. Goscianska, M.

- Kalmutzki, U. Lächelt, E. Ploetz, C. S. Diercks, S. Wuttke, *Angew. Chem., Int. Ed.* **2021**, *60*, 23975.
- [58] J. Andreo, R. Ettlinger, O. Zaremba, Q. Peña, U. Lächelt, R. F. de Luis, R. Freund, S. Canossa, E. Ploetz, W. Zhu, C. S. Diercks, H. Gröger, S. Wuttke, *J. Am. Chem. Soc.* **2022**, *144*, 7531.
- [59] S. Dutta, Y. D. More, S. Fajal, W. Mandal, G. K. Dam, S. K. Ghosh, *Chem. Commun.* **2022**, *58*, 13676.
- [60] S. Canossa, Z. Ji, C. Gropp, Z. Rong, E. Ploetz, S. Wuttke, O. M. Yaghi, *Nat. Rev. Mater.* **2022**, *8*, 331.
- [61] Z. Ji, H. Wang, S. Canossa, S. Wuttke, O. M. Yaghi, *Adv. Funct. Mater.* **2020**, *30*, 2000238.
- [62] E. Ploetz, H. Engelke, U. Lächelt, S. Wuttke, *Adv. Funct. Mater.* **2020**, *30*, 1909062.
- [63] F. Haase, P. Hirschle, R. Freund, S. Furukawa, Z. Ji, S. Wuttke, *Angew. Chem., Int. Ed.* **2020**, *59*, 22350.
- [64] S. Zhou, O. Shekhah, J. Jia, J. Czaban-Jóźwiak, P. M. Bhatt, A. Ramírez, J. Gascon, M. Eddaoudi, *Nat. Energy* **2021**, *6*, 882.
- [65] R. Vismara, S. Terruzzi, A. Maspero, T. Grell, F. Bossola, A. Sironi, S. Galli, J. A. R. Navarro, V. Colombo, *Adv. Mater.* **2023**, 2209907.
- [66] S. Yang, L. Peng, O. A. Syzgantseva, O. Trukhina, I. Kochetygov, A. Justin, D. T. Sun, H. Abedini, M. A. Syzgantseva, E. Oveisi, G. Lu, W. L. Queen, *J. Am. Chem. Soc.* **2020**, *142*, 13415.
- [67] V. V. Karve, N. A. Nekrasova, M. Asgari, O. Trukhina, I. V. Kochetygov, H. Abedini, S. Yang, E. V. Alexandrov, J. S. Luterbacher, W. L. Queen, *Chem. Mater.* **2022**, *34*, 9854.
- [68] R. Freund, S. Canossa, S. M. Cohen, W. Yan, H. Deng, V. Guillerme, M. Eddaoudi, D. G. Madden, D. Fairen-Jimenez, H. Lyu, L. K. Macreadie, Z. Ji, Y. Zhang, B. Wang, F. Haase, C. Woll, O. Zaremba, J. Andreo, S. Wuttke, C. S. Diercks, *Angew. Chem., Int. Ed.* **2021**, *60*, 23946.
- [69] H. Li, M. Eddaoudi, M. O'Keeffe, O. M. Yaghi, *Nature* **1999**, *402*, 276.
- [70] N. Hanikel, D. Kurandina, S. Chheda, Z. Zheng, Z. Rong, S. E. Neumann, J. Sauer, J. I. Siepmann, L. Gagliardi, O. M. Yaghi, *ACS Cent. Sci.* **2023**, *9*, 551.
- [71] Z. Zheng, N. Hanikel, H. Lyu, O. M. Yaghi, *J. Am. Chem. Soc.* **2022**, *144*, 22669.
- [72] S. M. Cohen, *J. Am. Chem. Soc.* **2017**, *139*, 2855.
- [73] W. Xu, O. M. Yaghi, *ACS Cent. Sci.* **2020**, *6*, 1348.
- [74] B. F. Hoskins, B. R. Robson, *J. Am. Chem. Soc.* **1990**, *112*, 1546.
- [75] E. D. Bloch, D. Britt, C. Lee, C. J. Doonan, F. J. U. Romo, H. Furukawa, J. R. Long, O. M. Yaghi, *J. Am. Chem. Soc.* **2010**, *132*, 14382.
- [76] A. Ejsmont, J. Andreo, A. Lanza, A. Galarda, L. Macreadie, S. Wuttke, S. Canossa, E. Ploetz, J. Goscianska, *Coord. Chem. Rev.* **2021**, *430*, 213655.
- [77] S. Mukherjee, S. Dutta, Y. D. More, S. Fajal, S. K. Ghosh, *Dalton Trans.* **2021**, *50*, 17832.
- [78] Y. Yao, C. Wang, J. Na, M. S. A. Hossain, X. Yan, H. Zhang, M. A. Amin, J. Qi, Y. Yamauchi, J. Li, *Small* **2022**, *18*, 2104387.
- [79] C. Wang, X. Liu, N. Keser Demir, J. P. Chen, K. Li, *Chem. Soc. Rev.* **2016**, *45*, 5107.
- [80] M. Kalaj, K. C. Bentz, S. Ayala Jr., J. M. Palomba, K. S. Barcus, Y. Katayama, S. M. Cohen, *Chem. Rev.* **2020**, *120*, 8267.
- [81] G. A. H. Sallam, E. A. Elsayed, *Ain Shams Eng. J.* **2018**, *9*, 1.
- [82] R. M. DuChanois, N. J. Cooper, B. Lee, S. K. Patel, L. Mazurowski, T. E. Graedel, M. Elimelech, *Nat. Water* **2023**, *1*, 37.
- [83] M. S. Diallo, M. R. Kotte, M. Cho, *Environ. Sci. Technol.* **2015**, *49*, 9390.
- [84] M. G. Buonomenna, *Symmetry* **2022**, *14*, 681.
- [85] D. T. Sun, N. Gasilova, S. Yang, E. Oveisi, W. L. Queen, *J. Am. Chem. Soc.* **2018**, *140*, 16697.
- [86] H. Liu, T. Fu, Y. Mao, *ACS Omega* **2022**, *7*, 14430.
- [87] A. Najim, *npj Clean Water* **2022**, *5*, 15.
- [88] W. J. Hahn, *Desalination* **1986**, *59*, 321.
- [89] A. Sonune, R. Ghate, *Desalination* **2004**, *167*, 55.
- [90] N. Kabay, M. Bryjak, S. Schlosser, M. Kitis, S. Avlonitis, Z. Matejka, I. Al-Mutaz, M. Yuksel, *Desalination* **2008**, *223*, 38.
- [91] N. Kabay, S. Sarp, M. Yuksel, Ö. Arar, M. Bryjak, *React. Funct. Polym.* **2007**, *67*, 1643.
- [92] R. F. Probst, *Physicochemical Hydrodynamics: An Introduction*, 2nd ed., Vol. XV, Wiley-Interscience, Hoboken, NJ **2003**, p. 400.
- [93] A. W. Mohammad, Y. H. Teow, W. L. Ang, Y. T. Chung, D. L. Oatley-Radcliffe, N. Hilal, *Desalination* **2015**, *356*, 226.
- [94] M. Qasim, M. Badrelzaman, N. N. Darwish, N. A. Darwish, N. Hilal, *Desalination* **2019**, *459*, 59.
- [95] N. Abdullah, N. Yusof, W. J. Lau, J. Jaafar, A. F. Ismail, *J. Ind. Eng. Chem.* **2019**, *76*, 17.
- [96] H. Choi, M. Son, H. Choi, *Chemosphere* **2017**, *185*, 1181.
- [97] L. Li, W. Shi, S. Yu, *Water* **2020**, *12*, 107.
- [98] B. L. Pangarkar, M. G. Sane, M. Guddad, *ISRN Mater. Sci.* **2011**, *2011*, 523124.
- [99] D. Gonzalez, J. Amigo, F. Suarez, *Renewable Sustainable Energy Rev.* **2017**, *80*, 238.
- [100] A. Alkhdhri, N. Darwish, N. Hilal, *Desalination* **2012**, *287*, 2.
- [101] N. Li, J. Xu, R. Feng, T.-L. Hu, X.-H. Bu, *Chem. Commun.* **2016**, *52*, 8501.
- [102] S. Dutta, P. Samanta, B. Joarder, S. Let, D. Mahato, R. Babarao, S. K. Ghosh, *ACS Appl. Mater. Interfaces* **2020**, *12*, 41810.
- [103] N. C. Burtch, H. Jajuja, K. S. Walton, *Chem. Rev.* **2014**, *114*, 10575.
- [104] J. Pei, K. Shao, L. Zhang, H. M. Wen, B. Li, G. Qian, *Top. Curr. Chem.* **2019**, *377*, 33.
- [105] C. Wang, X. Liu, N. K. Demir, J. P. Chen, K. Li, *Chem. Soc. Rev.* **2016**, *45*, 5107.
- [106] X. Sui, H. Ding, Z. Yuan, C. F. Leong, K. Goh, W. Li, N. Yang, D. M. D'Alessandro, Y. Chen, *Carbon* **2019**, *148*, 277.
- [107] A. Elrasheedy, N. Nady, M. Bassyouni, A. El-shazly, *Membranes* **2019**, *9*, 88.
- [108] M. S. Denny Jr., J. C. Moreton, L. Benz, S. M. Cohen, *Nat. Rev. Mater.* **2016**, *1*, 16078.
- [109] K. C. Bentz, K. Gnanasekaran, J. B. Bailey, S. Ayala Jr, F. A. Tezcan, N. C. Gianneschi, S. M. Cohen, *Chem. Sci.* **2020**, *11*, 10523.
- [110] G. I. Tovar, A. Valverde, C. Mendes-Felipe, S. Wuttke, A. Fidalgo-Marijuan, E. S. Larrea, L. Lezama, F. Zheng, J. Reguera, S. Lanceros-Méndez, M. I. Arriortua, G. Copello, R. F. de Luis, *Chem. - Eur. J.* **2021**, *14*, 2892.
- [111] F. Ahmadijokani, H. Molavi, M. Amini, A. Bahi, S. Wuttke, T. M. Aminabhavi, M. Kamkar, O. J. Rojas, F. Ko, M. Arjmand, *Chem. Eng. J.* **2023**, *466*, 143119.
- [112] F. Ahmadijokani, H. Molavi, A. Bahi, S. Wuttke, M. Kamkar, O. J. Rojas, F. Ko, M. Arjmand, *Chem. Eng. J.* **2023**, *457*, 141176.
- [113] S. Wang, J. S. Lee, M. Wahiduzzaman, J. Park, M. Muschi, C. Martineau-Corcoss, A. Tissot, K. H. Cho, J. Marrot, W. Shepard, G. Maurin, J.-S. Chang, C. Serre, *Nat. Energy* **2018**, *3*, 985.
- [114] G. Ghirlanda, *Nat. Chem.* **2021**, *13*, 621.
- [115] F. Li, G. Hanna, G. Yücesan, A. O. Yazaydin, *ACS Appl. Nano Mater.* **2023**, *6*, 3003.
- [116] J. Lu, X. Hu, K. M. Ung, Y. Zhu, X. Zhang, H. Wang, *Acc. Mater. Res.* **2022**, *3*, 735.
- [117] J. Lu, H. Zhang, J. Hou, X. Li, X. Hu, Y. Hu, C. D. Easton, Q. Li, C. Sun, A. W. Thornton, M. R. Hill, X. Zhang, G. Jiang, J. Z. Liu, A. J. Hill, B. D. Freeman, L. Jiang, H. Wang, *Nat. Mater.* **2020**, *19*, 767.
- [118] C. Gropp, S. Canossa, S. Wuttke, F. Gándara, Q. Li, L. Gagliardi, O. M. Yaghi, *ACS Cent. Sci.* **2020**, *6*, 1255.
- [119] J. Lu, H. Zhang, X. Hu, B. Qian, J. Hou, L. Han, Y. Zhu, C. Sun, L. Jiang, H. Wang, *ACS Nano* **2021**, *15*, 1240.
- [120] R. Jamshidi Gohari, W. J. Lau, T. Matsuura, A. F. Ismail, *Sep. Purif. Technol.* **2013**, *118*, 64.



- [121] H. Wang, S. Zhao, Y. Liu, R. Yao, X. Wang, Y. Cao, D. Ma, M. Zou, A. Cao, X. Feng, B. Wang, *Nat. Commun.* **2019**, *10*, 4204.
- [122] H. Fan, Q. Shi, H. Yan, S. Ji, J. Dong, G. Zhang, *Angew. Chem., Int. Ed.* **2014**, *53*, 5578.
- [123] R. Zhang, S. Ji, N. Wang, L. Wang, G. Zhang, J. R. Li, *Angew. Chem., Int. Ed.* **2014**, *53*, 9775.
- [124] X. Liu, N. K. Demir, Z. Wu, K. Li, *J. Am. Chem. Soc.* **2015**, *137*, 6999.
- [125] Z. Li, G. Zhou, H. Dai, M. Yang, Y. Fu, Y. Ying, Y. Li, *J. Mater. Chem. A* **2108**, *6*, 3402.
- [126] J. E. Efome, D. Rana, T. Matsuura, C. Q. Lan, *ACS Appl. Mater. Interfaces* **2018**, *10*, 18619.
- [127] W. J. Lau, A. F. Ismail, P. S. Goh, N. Hilal, B. S. Ooi, *Sep. Purif. Rev.* **2015**, *44*, 135.
- [128] J. Polte, *CrystEngComm* **2015**, *17*, 6809.
- [129] R. Freund, U. Lächelt, T. Gruber, B. Rühle, S. Wuttke, *ACS Nano* **2018**, *12*, 2094.
- [130] P. Hirschle, C. Hirschle, K. Böll, M. Döblinger, M. Höhn, J. M. Tuffnell, C. W. Ashling, D. A. Keen, T. D. Bennett, J. O. Rädler, E. Wagner, M. Peller, U. Lächelt, S. Wuttke, *Chem. Mater.* **2020**, *32*, 2253.
- [131] P. Hirschle, T. Preiß, F. Auras, A. Pick, J. Völkner, D. Valdepérez, G. Witte, W. J. Parak, J. O. Rädler, S. Wuttke, *CrystEngComm* **2016**, *18*, 4359.
- [132] M. M. Modena, B. Rühle, T. P. Burg, S. Wuttke, *Adv. Mater.* **2019**, *31*, 1901556.
- [133] L. Liu, Z.-P. Tao, H.-R. Chi, B. Wang, S.-M. Wang, Z.-B. Han, *Dalton Trans.* **2021**, *50*, 39.
- [134] O. M. Yaghi, G. Li, H. Li, *Nature* **1995**, *378*, 703.
- [135] S. Cong, Y. Yuan, J. Wang, Z. Wang, F. Kapteijn, X. Liu, *J. Am. Chem. Soc.* **2021**, *143*, 20055.
- [136] X. Dong, Y. S. Lin, *Chem. Commun.* **2013**, *49*, 1196.
- [137] R. Ou, H. Zhang, V. X. Truong, L. Zhang, H. M. Hegab, L. Han, J. Hou, X. Zhang, A. Deletic, L. Jiang, G. P. Simon, H. Wang, *Nat. Sustain.* **2020**, *3*, 1052.
- [138] J. Zhu, L. Qin, A. Uliana, J. Hou, J. Wang, Y. Zhang, X. Li, S. Yuan, J. Li, M. Tian, J. Lin, B. Van der Bruggen, *ACS Appl. Mater. Interfaces* **2017**, *9*, 1975.
- [139] S. Hermes, F. Schröder, R. Chelmowski, C. Wöll, R. A. Fischer, *J. Am. Chem. Soc.* **2005**, *127*, 13744.
- [140] Y. Liu, Z. Ng, E. A. Khan, H.-K. Jeong, C.-b. Ching, Z. Lai, *Micropor. Mesopor. Mat.* **2009**, *118*, 296.
- [141] A. Centrone, Y. Yang, S. Speakman, L. Bromberg, G. C. Rutledge, T. A. Hatton, *J. Am. Chem. Soc.* **2010**, *132*, 15687.
- [142] Y. Hu, X. Dong, J. Nan, W. Jin, X. Ren, N. Xu, Y. M. Lee, *Chem. Commun.* **2011**, *47*, 737.
- [143] Y. Pan, T. Li, G. Lestari, Z. Lai, *J. Membr. Sci.* **2012**, *390–391*, 93.
- [144] Y. Peng, Y. Li, Y. Ban, H. Jin, W. Jiao, X. Liu, W. Yang, *Science* **2014**, *346*, 1356.
- [145] Q. Li, L. Cheng, J. Shen, J. Shi, G. Chen, J. Zhao, J. Duan, G. Liu, W. Jin, *Sep. Purif. Technol.* **2017**, *178*, 105.
- [146] T.-Y. Liu, H.-G. Yuan, Y.-Y. Liu, D. Ren, Y.-C. Su, X. Wang, *ACS Nano* **2018**, *12*, 9253.
- [147] Y. Wang, X. Li, S. Zhao, Z. Fang, D. Ng, C. Xie, H. Wang, Z. Xie, *Ind. Eng. Chem. Res.* **2019**, *58*, 195.
- [148] X.-Y. Gong, Z.-H. Huang, H. Zhang, W.-L. Liu, X.-H. Ma, Z.-L. Xu, C. Y. Tang, *Chem. Eng. J.* **2020**, *398*, 125706.
- [149] X. Li, Y. Liu, J. Wang, J. Gascon, J. Li, B. Van der Bruggen, *Chem. Soc. Rev.* **2017**, *46*, 7124.
- [150] Z. Kang, M. Xue, L. Fan, J. Ding, L. Guo, L. Gao, S. Qiu, *Chem. Commun.* **2013**, *49*, 10569.
- [151] Y. Zhu, K. M. Gupta, Q. Liu, J. Jiang, J. Caro, A. Huang, *Desalination* **2016**, *385*, 75.
- [152] J. Yuan, W.-S. Hung, H. Zhu, K. Guan, Y. Ji, Y. Mao, G. Liu, K.-R. Lee, W. Jin, *J. Membr. Sci.* **2019**, *572*, 20.
- [153] O. Shekhah, H. Wang, S. Kowarik, F. Schreiber, M. Paulus, M. Tolan, C. Sternemann, F. Evers, D. Zacher, R. A. Fischer, C. Woll, *J. Am. Chem. Soc.* **2007**, *129*, 15118.
- [154] L. Wang, M. Fang, J. Liu, J. He, J. Li, J. Lei, *ACS Appl. Mater. Interfaces* **2015**, *7*, 24082.
- [155] J. Liu, F. Yang, Q. L. Zhang, W. Chen, Y. F. Gu, Q. Chen, *Inorg. Chem.* **2019**, *58*, 3564.
- [156] S. Sorribas, P. Gorgojo, C. Tellez, J. Coronas, A. G. Livingston, *J. Am. Chem. Soc.* **2013**, *135*, 15201.
- [157] D. Ma, S. B. Peh, G. Han, S. B. Chen, *ACS Appl. Mater. Interfaces* **2017**, *9*, 7523.
- [158] A. Zirehpour, A. Rahimpour, M. Ulbricht, *J. Membr. Sci.* **2017**, *531*, 59.
- [159] Z. P. Liao, X. F. Fang, J. Xie, Q. Li, D. P. Wang, X. Y. Sun, L. J. Wang, J. S. Li, *ACS Appl. Mater. Interfaces* **2019**, *11*, 5344.
- [160] Y. Y. Zhao, Y. L. Liu, X. M. Wang, X. Huang, Y. F. Xie, *ACS Appl. Mater. Interfaces* **2019**, *11*, 13724.
- [161] a) Q. Li, J. S. Li, X. F. Fang, Z. P. Liao, D. P. Wang, X. Y. Sun, J. Y. Shen, W. Q. Han, L. J. Wang, *Chem. Commun.* **2018**, *54*, 3590; b) Y. Li, L. H. Wee, A. Volodin, J. A. Martens, I. F. J. Vankelecom, *Chem. Commun.* **2015**, *51*, 918.
- [162] J. Dechnik, J. Gascon, C. J. Doonan, C. Janiak, C. J. Sumbly, *Angew. Chem., Int. Ed.* **2017**, *56*, 9292.
- [163] X. L. Liu, Y. S. Li, G. Q. Zhu, Y. J. Ban, L. Y. Xu, W. S. Yang, *Angew. Chem., Int. Ed.* **2011**, *50*, 10636.
- [164] X.-H. Ma, Z. Yang, Z.-K. Yao, Z.-L. Xua, C. Y. Tang, *J. Membr. Sci.* **2017**, *525*, 269.
- [165] Y. Lin, H. C. Wu, T. Yasui, T. Yoshioka, H. Matsuyama, *ACS Appl. Mater. Interfaces* **2019**, *11*, 18782.
- [166] Z. Huang, G. Yang, J. Zhang, S. Gray, Z. Xie, *Desalination* **2021**, *518*, 115268.
- [167] J. Zuo, T.-S. Chung, *Water* **2016**, *8*, 586.
- [168] H. Mao, H.-G. Zhen, A. Ahmad, A.-S. Zhang, Z.-P. Zhao, *J. Membr. Sci.* **2019**, *573*, 344.
- [169] C. H. Wang, C. Liu, J. S. Li, X. Y. Sun, J. Y. Shen, W. Q. Han, L. J. Wang, *Chem. Commun.* **2017**, *53*, 1751.
- [170] Z. Zhou, X.-F. Wu, *Mater. Lett.* **2015**, *160*, 423.
- [171] F. Yang, J. E. Efome, D. Rana, T. Matsuura, C. Lan, *ACS Appl. Mater. Interfaces* **2018**, *10*, 11251.
- [172] W.-S. Hung, Q.-F. An, M. De Guzman, H.-Y. Lin, S.-H. Huang, W.-R. Liu, C.-C. Hu, K.-R. Lee, J.-Y. Lai, *Carbon* **2014**, *68*, 670.
- [173] J. F. Yao, D. H. Dong, D. Li, L. He, G. S. Xu, H. T. Wang, *Chem. Commun.* **2011**, *47*, 2559.
- [174] Y. F. Chen, S. Q. Li, X. K. Pei, J. W. Zhou, X. Feng, S. H. Zhang, Y. Y. Cheng, H. W. Li, R. D. Han, B. Wang, *Angew. Chem., Int. Ed.* **2016**, *55*, 3419.
- [175] X. J. Ma, Y. T. Chai, P. Li, B. Wang, *Acc. Chem. Res.* **2019**, *52*, 1461.
- [176] W. Li, P. Su, Z. Li, Z. Xu, F. Wang, H. Ou, J. Zhang, G. Zhang, E. Zeng, *Nat. Commun.* **2017**, *8*, 406.
- [177] S. Porada, R. Zhao, A.v.d. Wal, V. Presser, P. M. Biesheuvel, *Prog. Mater. Sci.* **2013**, *58*, 1388.
- [178] K. Foo, B. Hameed, *J. Hazard. Mater.* **2009**, *170*, 552.
- [179] M. S. Gaikwad, C. Balomajumder, *Anal. Lett.* **2016**, *49*, 1641.
- [180] Y. Li, J. Shen, J. Li, X. Sun, J. Shen, W. Han, L. Wang, *Carbon* **2017**, *116*, 21.
- [181] X. Xu, A. E. Allah, C. Wang, H. Tan, A. A. Farghali, M. H. Khedr, V. Malgras, T. Yang, Y. Yamauchi, *Chem. Eng. J.* **2019**, *362*, 887.
- [182] X. Xu, H. Tan, Z. Wang, C. Wang, L. Pan, Y. V. Kaneti, T. Yang, Y. Yamauchi, *Environ. Sci.: Nano* **2019**, *6*, 981.
- [183] K. Shi, I. Zhitomirsky, *Electrochim. Acta* **2015**, *174*, 588.
- [184] K. Shi, M. Ren, I. Zhitomirsky, *ACS Sustainable Chem. Eng.* **2014**, *2*, 1289.
- [185] K. Shi, X. Yang, E. D. Cranston, I. Zhitomirsky, *Adv. Funct. Mater.* **2016**, *26*, 6437.

- [186] X. Yang, K. Shi, I. Zhitomirsky, E. D. Cranston, *Adv. Mater.* **2015**, *27*, 6104.
- [187] I. Cohen, E. Avraham, Y. Bouhadana, A. Soffer, D. Aurbach, *Electrochim. Acta* **2013**, *106*, 91.
- [188] Z. Wang, X. Xu, J. Kim, V. Malgras, R. Mo, C. Lo, Y. Lin, H. Tan, J. Tang, L. Pan, Y. Bando, T. Yang, Y. Yamauchi, *Mater. Horiz.* **2019**, *6*, 1433.
- [189] M. Ding, W. Shi, Z. Leong, L. Guo, A. Baji, H. Y. Yang, *J. Mater. Chem.* **2017**, *5*, 6113.
- [190] T. Y. Cath, A. E. Childress, M. Elimelech, *J. Membr. Sci.* **2006**, *281*, 70.
- [191] S. Xiong, J. Zuo, Y. G. Ma, L. Liu, H. Wu, Y. Wang, *J. Membr. Sci.* **2016**, *520*, 400.
- [192] D. L. Shaffer, J. R. Werber, H. Jaramillo, S. Lin, M. Elimelech, *Desalination* **2015**, *356*, 271.
- [193] S. Loeb, S. Sourirajan, *Adv. Chem.* **1963**, *9*, 117.
- [194] P. Vandezane, L. E. M. Gevers, I. F. J. Vankelecom, *Chem. Soc. Rev.* **2008**, *37*, 365.
- [195] D. Ma, S. B. Peh, G. Han, S. B. Chen, D. Ma, S. B. Peh, G. Han, S. B. Chen, *ACS Appl. Mater. Interfaces* **2017**, *9*, 7523.
- [196] R. Dai, X. Zhang, M. Liu, Z. Wu, Z. Wang, *J. Membr. Sci.* **2019**, *573*, 46.
- [197] J. J. Beh, B. S. Ooi, J. K. Lim, E. P. Ng, H. Mustapa, *J. Water Process. Eng.* **2020**, *33*, 101031.
- [198] J. W. Wu, M. J. Biggs, E. J. Hua, *Chem. Eng. Res. Des.* **2010**, *88*, 1541;
- [199] E. Elsayed, R. Al-dadah, S. Mahmoud, P. A. Anderson, A. Elsayed, P. G. Youssef, *Desalination* **2016**, *406*, 25.
- [200] H. Kim, H. J. Cho, S. Narayanan, S. Yang, H. Furukawa, S. Schiffrés, X. Li, Y.-B. Zhang, J. Jiang, O. M. Yaghi, E. N. Wang, *Sci. Rep.* **2016**, *6*, 19097.
- [201] S. Lin, M. Elimelech, *Desalination* **2017**, *401*, 42.
- [202] Z. Hu, Y. Chen, J. Jiang, *J. Chem. Phys.* **2011**, *134*, 134705.
- [203] K. M. Gupta, K. Zhang, J. Jiang, *Langmuir* **2015**, *31*, 13230.
- [204] J. Duan, Y. Pan, F. Pacheco, E. Litwiller, Z. Lai, I. Pinnau, *J. Membr. Sci.* **2015**, *476*, 303.
- [205] T. H. Lee, J. Y. Oh, S. P. Hong, J. M. Lee, S. M. Roh, S. H. Kim, H. B. Park, *J. Membr. Sci.* **2019**, *570-571*, 23.
- [206] I. H. Aljundi, *Desalination* **2017**, *420*, 12.
- [207] Y. Xu, X. Gao, X. X. Wang, Q. Wang, Z. Ji, X. X. Wang, T. Wu, C. Gao, *Materials* **2016**, *9*, 870.
- [208] B. L. Bonnett, E. D. Smith, M. De La Garza, M. Cai, J. V. Haag, J. M. Serrano, H. D. Cornell, B. Gibbons, S. M. Martin, A. J. Morris, *ACS Appl. Mater. Interfaces* **2020**, *12*, 15765.
- [209] H. M. Park, K. Y. Jee, Y. T. Lee, *J. Membr. Sci.* **2017**, *541*, 510.
- [210] Y. Lin, Y. Chen, R. Wang, *J. Membr. Sci.* **2019**, *589*, 117249.
- [211] E. Drioli, A. Ali, F. Macedonia, *Desalination* **2014**, *356*, 56.
- [212] D. Cheng, L. Zhao, N. Li, S. J. D. Smith, D. Wu, J. Zhang, D. Ng, C. Wu, M. R. Martinez, M. P. Batten, Z. Xie, *J. Membr. Sci.* **2019**, *588*, 117204.
- [213] M. R. S. Kebría, A. Rahimour, G. Bakéri, R. Abedini, *Desalination* **2019**, *450*, 21.
- [214] Y. Li, L. H. Wee, J. A. Martens, I. F. J. Vankelecom, *J. Membr. Sci.* **2017**, *523*, 561.
- [215] H. Liu, M. Zhang, H. Zhao, Y. Jiang, G. Liu, J. Gao, *RSC Adv.* **2020**, *10*, 4045.
- [216] M. Navarro, J. Benito, L. Paseta, I. Gascón, J. Coronas, C. T´ellez, *ACS Appl. Mater. Interfaces* **2018**, *10*, 1278.
- [217] J. Zhu, J. Hou, S. Yuan, Y. Zhao, Y. Li, R. Zhang, M. Tian, J. Li, J. Wang, B. Van Der Bruggen, *J. Mater. Chem. A* **2019**, *7*, 16313.
- [218] Z. Wang, Z. Wang, S. Lin, H. Jin, S. Gao, Y. Zhu, J. Jin, *Nat. Commun.* **2018**, *9*, 2004.
- [219] M. Jian, R. Qiu, Y. Xia, J. Lu, Y. Chen, Q. Gu, R. Liu, C. Hu, J. Qu, H. Wang, X. Zhang, *Sci. Adv.* **2020**, *6*, eaay3998.
- [220] Y. Wen, R. Dai, X. Li, X. Zhang, X. Cao, Z. Wu, S. Lin, C. Y. Tang, Z. Wang, *Sci. Adv.* **2022**, *8*, eabm4149.
- [221] Y. Xu, X. Gao, X. Wang, Q. Wang, Z. Ji, X. Wang, T. Wu, C. Gao, *Materials* **2016**, *9*, 870.
- [222] M. Kadhon, W. Hu, B. Deng, *Membranes* **2017**, *7*, 31.
- [223] Y. He, Y. P. Tang, D. Ma, T. S. Chung, *J. Membr. Sci.* **2017**, *541*, 262.
- [224] J. Park, Q. Jiang, D. Feng, L. Mao, H. C. Zhou, *J. Am. Chem. Soc.* **2016**, *138*, 3518.
- [225] N. Misdan, N. Ramlee, N. H. H. Hairom, S. N. W. Ikhsan, N. Yusuf, W. J. Lau, A. F. Ismail, N. A. H. M. Nordin, *Chem. Eng. Res. Des.* **2019**, *148*, 227.
- [226] H. Daglar, C. Altintas, I. Erucar, G. Heidari, E. N. Zare, O. Moradi, V. Srivastava, S. Iftekhar, S. Keskin, M. Sillanpaa, *Chemosphere* **2022**, *303*, 135082.



**Subhajt Dutta** obtained his BSc (Chemistry) from the University of Calcutta in 2014 and MSc (Chemistry) from the University of Calcutta in 2016. Thereafter, he joined the Indian Institute of Science Education and Research (IISER), Pune as a Ph.D. student under the supervision of Prof. Sujit K. Ghosh and completed his Ph.D. in 2022. Subsequently, Subhajt joined BCMaterials (Basque Center for Materials, Applications and Nanostructures, Spain) to pursue his post-doctoral research work under Prof. Stefan Wuttke. His current research interests embrace the development of next-generation functional porous materials that foster environmental sustainability.



**Stefan Wuttke** created the research group “WuttkeGroup for Science,” initially hosted at the Institute of Physical Chemistry at the University of Munich (LMU, Germany). Currently, he is an Ikerbasque Professor at the Basque Center for Materials, Applications, and Nanostructures (BCMaterials, Spain). His principal focus is the design, synthesis, and functionalization of MOFs and their nanometric counterparts to target diverse applications. At the same time, he aims to establish a basic understanding of the chemical and physical elementary processes involved in the synthesis, functionalization, and application of these hybrid materials.